

# Converting Divergent Weak-Coupling into Exponentially Fast Convergent Strong-Coupling Expansions

Hagen Kleinert

*Institut for Theoretical Physics, Free University Berlin, Berlin, Germany*

---

## Abstract

With the help of a simple variational procedure it is possible to convert the partial sums of order  $N$  of many divergent series expansions  $f(g) = \sum_{n=0}^{\infty} a_n g^n$  into partial sums  $\sum_{n=0}^N b_n g^{-\omega n}$ , where  $0 < \omega < 1$  is a parameter that parametrizes the approach to the large- $g$  limit. The latter are partial sums of a strong-coupling expansion of  $f(g)$  which converge against  $f(g)$  for  $g$  outside a certain divergence radius. The error decreases exponentially fast for large  $N$ , like  $e^{-\text{const.} \times N^{1-\omega}}$ . We present a review of the method and various applications.

**Keywords:** strong-coupling expansions, asymptotic series; resummation; critical exponents, non-Borel series.

**2000 MSC:** 34E05

---

## 1. Introduction

Variational techniques have a long history in theoretical physics. On the one hand, they serve to find equations of motion from the extrema of actions. On the other hand they help finding approximate solutions of physical problems by extremizing energies. In quantum mechanics, the Rayleigh-Ritz variational principle according to which the ground state energy of a system is bounded above by the inequality

$$E_0 \leq \int d^3x \psi^*(x) \hat{H} \psi(x) \quad (1)$$

has yielded many useful results. In many-body physics, the Hartree-Fock method has helped understanding electrons in metals and nuclear matter. In quantum field theory the effective action approach [1] has contributed greatly to the theory of phase transitions. In particular the higher effective actions pioneered by Dominicis [2].

A variational method was very useful in solving functional integrals of complicated quantum statistical systems, for instance the polaron problem [3]. Here another inequality plays an important role, the Jensen-Peierls inequality, according to which the expectation value of an exponential of a functional of a functional is at least as large as the exponential of the expectation value itself:

$$\langle e^{-O} \rangle \geq e^{-\langle O \rangle}. \quad (2)$$

This technique was extended in 1986 to find approximate solutions for the functional integrals of many other quantum mechanical systems [4].

An important progress was reached in 1993 by finding a way of applying the technique to arbitrarily high order [5]. The technique was developed further in the textbook [6]. This made it possible to perform the approximate calculation to any desired degree of accuracy. In contrast to the higher effective action approach, the treatment converged exponentially fast also in the strong-coupling limit [7].

---

*Email address:* h.k@fu-berlin.de (Hagen Kleinert)

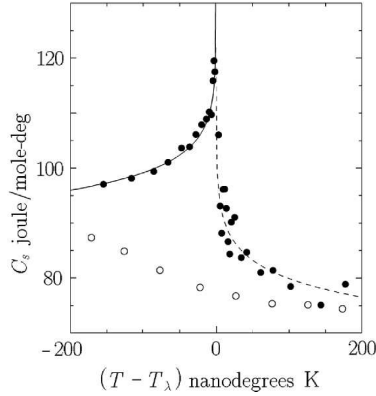


Figure 1: Experimental data of space shuttle experiment by Lipa et al. [8].

The zero-temperature version of this technique led to a new solution of an old problem in mathematical physics, that the results of many calculations can be given only in the form of divergent weak-coupling expansions. For instance, the energy eigenvalues  $E$  of a Schrödinger equation of a point particle of mass  $m$

$$\left[ -\hbar^2 \frac{\partial^2}{2M} + V(\mathbf{x}) \right] \psi(x) = E\psi(x) \quad (3)$$

moving in a three-dimensional potential

$$V(x) = \frac{\omega^2}{2} x^2 + gx^4 \quad (4)$$

can be given as a series in  $g/\omega^3$

$$E = \omega \left[ \sum_{n=0}^N a_n \left( \frac{g}{\omega} \right)^n \right]. \quad (5)$$

The coefficients  $a_n$  grow exponentially fast with  $n$ . The series has a zero radius of convergence. For the ground state it reads

$$E = \omega \left[ \frac{1}{2} + \frac{3}{4} \frac{g}{4\omega^3} - \frac{21}{8} \left( \frac{g}{4\omega^3} \right)^2 + \frac{333}{16} \left( \frac{g}{4\omega^3} \right)^3 + \dots \right]. \quad (6)$$

There exist similar divergent expansions for critical exponents which may be calculated from weak-coupling expansions of quantum field theories and are experimentally measurable near second-order phase transitions. One of these is the exponents  $\alpha$  which determines the behavior of the specific heat of superfluid helium near the phase transition to the normal fluid. It has been measured with extreme accuracy in a recent satellite experiment [8]. The result agrees very well with the value of the series for  $\alpha$  as a power series in  $g/m$  in the strong-coupling limit  $m \rightarrow 0$  [24]

In many more physical examples the properties are found by evaluating divergent weak-coupling series in the strong coupling limit.

In this lecture I shall present the main ideas and sketch a few applications of *Variational Perturbation Theory*.

## 2. Quantum Mechanical Example

In order to illustrate the method let us obtain the strong-coupling value of the ground state energy (6). We introduce a dummy variational parameter by the substitution

$$\omega \rightarrow \sqrt{\Omega^2 + (\omega^2 - \Omega^2)} \equiv \sqrt{\Omega^2 + gr}, \quad (7)$$

where  $r$  is short for

$$r \equiv (\omega^2 - \Omega^2)/g. \quad (8)$$

This substitution does not change the partial sums of series (6):

$$E^N = \omega \sum_{n=0}^N a_n \left( \frac{g}{4\omega^3} \right)^n \quad (9)$$

for any order  $N$ . If we, however, re-expand these partial sums in powers of  $g$  at fixed  $r$  up to order  $N$ , and substitute at the end  $r$  by  $(\omega^2 - \Omega^2)/g$ , we obtain new partial sums

$$W^N = \Omega \sum_{n=0}^N a'_n \left( \frac{g}{\Omega^3} \right)^n. \quad (10)$$

In contrast to  $E^N$ , these *do depend* on the variational parameter  $\Omega$ . For higher and higher orders, the  $\Omega$ -dependence has an increasing valley where the dependence is very weak. It can be found analytically by setting the first derivative equal to zero, or, if this equation has no solution, by setting the second derivative equal to zero. One may view this as a manifestation of a *principle of minimal sensitivity* [10]. The plots are shown in Fig. 2 for odd  $N$  and even  $N$ .

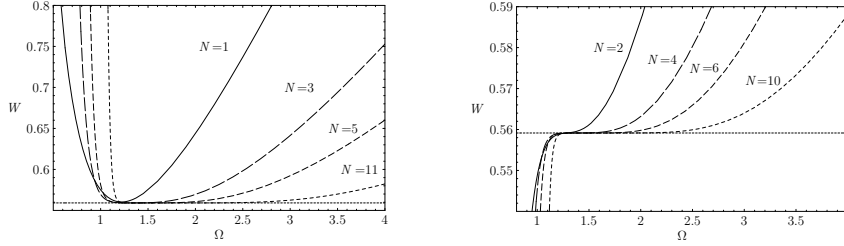


Figure 2: Typical  $\Omega$ -dependence of  $N$ th approximations  $W_N$  at  $T = 0$  for increasing orders  $N$ . The coupling constant has the value  $g/4 = 0.1$ . The dashed horizontal line indicates the exact energy.

Even to lowest order, the result is surprisingly accurate. For  $N = 1$ , the energy  $E^N$  we have the linear dependence

$$E^1 = \omega \left( \frac{1}{2} + \frac{3}{16} \frac{g}{\omega^3} \right). \quad (11)$$

After the replacement (7) and the reexpansion up to power  $g$  at fixed  $r$  we find

$$W^1 = \Omega \left( \frac{1}{4} + \frac{\omega^2}{4\Omega} + \frac{3}{16} \frac{g}{\Omega^4} \right). \quad (12)$$

In the strong-coupling limit, the minimum lies at  $\Omega \approx c(g/4)^{1/3}$  where  $c$  is some constant and the energy behaves like

$$W^1 \approx \left( \frac{g}{4} \right)^{1/3} \left( \frac{c}{4} + \frac{3}{4c^2} \right). \quad (13)$$

The minimum lies at  $c = 6^{1/3}$  where  $W^1 \approx (g/4)^{1/3} (3/4)^{4/3} \approx (g/4)^{1/3} \times 0.681420$ . The treatment can easily be extended to 40 digits [11] starting out like  $E^1 = (g/4)^{1/3} \times 0.667\,986\,259 \dots$ .

The result is shown in for  $g/4 = 0.1$  in Fig. 3. If we plot the minimum as a function of  $g$  we obtain the curve shown in Fig. 3. The curve has the asymptotic behavior  $(g/4)^{1/3} \times 0.68142$ . This grows with the *exact* power of  $g$  and has a coefficient that differs only slightly from the accurate value  $0.667\,986\,259 \dots$  found by other approximation procedures [12].

The convergence of the approximations is exponential as was shown in Refs. [13, 14, 15] using the technique of order-dependent mapping [17]. If the asymptotic behavior of  $E^N(g)$  and its variational approximation  $W^N(g)$  are parametrized by

$$W^N(g) = g^{1/3} \left\{ b_0 + b_1 g^{-2/3} + b_2 g^{-4/3} + \dots \right\}, \quad (14)$$

the coefficients  $b_0$  and  $b_1$  converge with  $N$  as shown in Fig. 4. The approach is oscillatory (see Fig. 5).

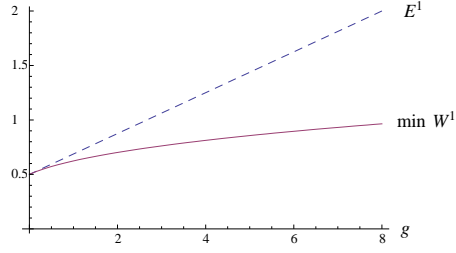


Figure 3: First-order perturbative energy  $E^1$  and the variational-perturbative minimum of  $W^1$ . The exact result follows closely the curve  $\min W^1$ .

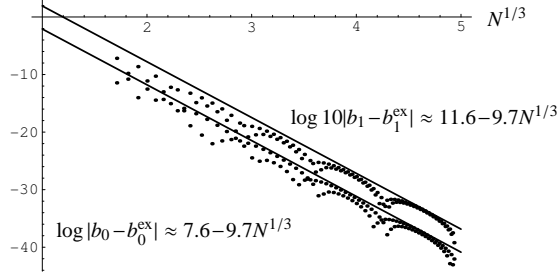


Figure 4: Asymptotic coefficients  $b_0$  and  $b_1$  of  $W^N$  as a function of the order  $N$ .

### 3. Quantum Field Theory and Critical Behavior

When trying to apply the same procedure to quantum field theory, the above procedure needs some important modification caused by the fact that the scaling dimensions of fields are no longer equal to the naive dimensions but *anomalous*. This causes the principle of minimal sensitivity to fail [16]. The adaption of the variational procedure was done in the textbook [18]. Let us briefly summarize it using an important class of field theories.

The energy is an  $O(n)$ -symmetric coupling functional of a  $n$ -component field  $\phi_0$  in  $D$  dimensions

$$E[\phi_0] = \int d^D x \left\{ \frac{1}{2} [\partial \phi_0(\mathbf{x})]^2 + \frac{m_0^2}{2} \phi_0(\mathbf{x})^2 + \frac{g_0}{4!} [\phi_0(\mathbf{x})^2]^2 \right\}, \quad (15)$$

where the parameters depend on the distance of the temperature from the critical value  $T_c$ :

$$m_0^2 = O((T - T_c)^1), \quad g_0 = O((T - T_c)^0)$$

The important critical behavior is seen in the correlation function which have the limiting form

$$\langle \phi_i(\mathbf{x}) \phi_j(\mathbf{x}') \rangle \sim \frac{e^{-|\mathbf{x} - \mathbf{x}'|/\xi(T)}}{|\mathbf{x} - \mathbf{x}'|^{D-2+\eta}}. \quad (16)$$

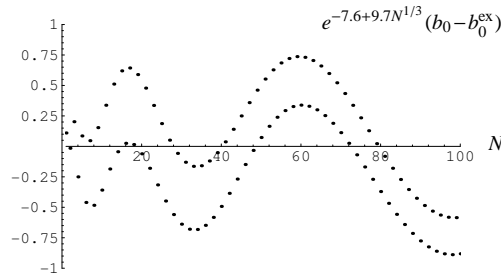


Figure 5: Oscillations of the strong-coupling coefficient  $b_0$ .

where  $\eta$  is the anomalous field dimension, and  $\xi$  is the coherence length which diverges near  $T_c$  like  $\xi(T) \sim (T - T_c)^{-\nu}$ .

### 3.1. Critical Behavior in $D - \epsilon$ Dimensions

The field fluctuations cause divergencies which can be removed by a renormalization of field, mass and coupling constant to  $\phi$ ,  $m$ , and  $g$ . This is most elegantly done by assuming the dimension of spacetime to be  $D = 4 - \epsilon$ , in which case the renormalization factor are

$$g_0 = Z_g(g, \epsilon) Z_\phi(g, \epsilon)^{-2} \mu^\epsilon g, \quad (17)$$

$$m_0^2 = Z_m(g, \epsilon) Z_\phi(g, \epsilon)^{-1} m^2, \quad (18)$$

$$\phi_0^2 = Z_\phi(g, \epsilon) \phi^2. \quad (19)$$

The factors have weak-coupling expansions:

$$Z_g(g, \epsilon) = 1 + \frac{n+8}{3\epsilon} g + \left\{ \frac{(n+8)^2}{9\epsilon^2} - \frac{5n+22}{9\epsilon} \right\} g^2 + \dots, \quad (20)$$

$$Z_\phi(g, \epsilon) = 1 - \frac{n+2}{36\epsilon} g^2 + \dots, \quad (21)$$

$$Z_m(g, \epsilon) = 1 + \frac{n+2}{3\epsilon} g + \left\{ \frac{(n+2)(n+5)}{9\epsilon^2} - \frac{n+2}{6\epsilon} \right\} g^2 + \dots.$$

The dependence of these on the scale parameter  $\mu$  defines the renormalization group functions

$$\beta(g, \epsilon) = \mu \left. \frac{dg}{d\mu} \right|_0 = -\epsilon \left\{ \frac{\partial}{\partial g} \ln [g Z_g(g, \epsilon) Z_\phi(g, \epsilon)^{-2}] \right\}^{-1}, \quad (22)$$

$$\gamma_m(g) = \frac{\mu}{m} \left. \frac{dm}{d\mu} \right|_0 = -\frac{\beta(g, \epsilon)}{2} \frac{\partial}{\partial g} \ln [Z_m(g, \epsilon) Z_\phi(g, \epsilon)^{-1}], \quad (23)$$

$$\gamma(g) = -\frac{\mu}{\phi} \left. \frac{d\phi}{d\mu} \right|_0 = \frac{\beta(g, \epsilon)}{2} \frac{\partial}{\partial g} \ln Z_\phi(g, \epsilon). \quad (24)$$

At the phase transition  $g_0$  goes to the strong-coupling limit  $g_0 \rightarrow \infty$ . In this limit the renormalized coupling  $g$  tends to a constant  $g^*$ , called the fixed point of the theory.

From the renormalization group functions in the strong-coupling limit one finds the physical observables at the critical point

$$\eta = 2\gamma(g^*) = \frac{n+2}{2(n+8)^2} \epsilon^2 + \dots, \quad (25)$$

$$\nu = \frac{1}{2[1 - \gamma_m(g^*)]} = \frac{1}{2} + \frac{n+2}{4(n+8)} \epsilon + \frac{(n+2)(n+3)(n+20)}{8(n+8)^3} \epsilon^2 + \dots, \quad (26)$$

$$\omega = \beta'(g^*, \epsilon) = \epsilon - \frac{3(3n+14)}{(n+8)^2} \epsilon^2 + \dots. \quad (27)$$

The quantity  $\epsilon$  is the so-called *anomalous dimension* of the field  $\phi(x)$ .

The  $\epsilon$ -expansions are divergent and are typically evaluated at the physical value  $\epsilon = 1$  where  $D = 3$  by various resummation procedures [19].

In variational perturbation theory the procedure is different. One rewrites the power series of Eq. (17) as of the renormalized coupling  $g_0$ :

$$g(g_0) = g_0 - \frac{n+8}{3\epsilon} g_0^2 + \left\{ \frac{(n+8)^2}{9\epsilon^2} + \frac{9n+42}{18\epsilon} \right\} g_0^3 + \dots. \quad (28)$$

For the dependence of the renormalized mass on the bare coupling one finds from Eq. (18)

$$\frac{m^2(g_0)}{m_0^2} = 1 - \frac{n+2}{3\epsilon} g_0 + \left\{ \frac{(n+2)(n+5)}{9\epsilon^2} + \frac{5(n+2)}{36\epsilon} \right\} g_0^2 + \dots. \quad (29)$$

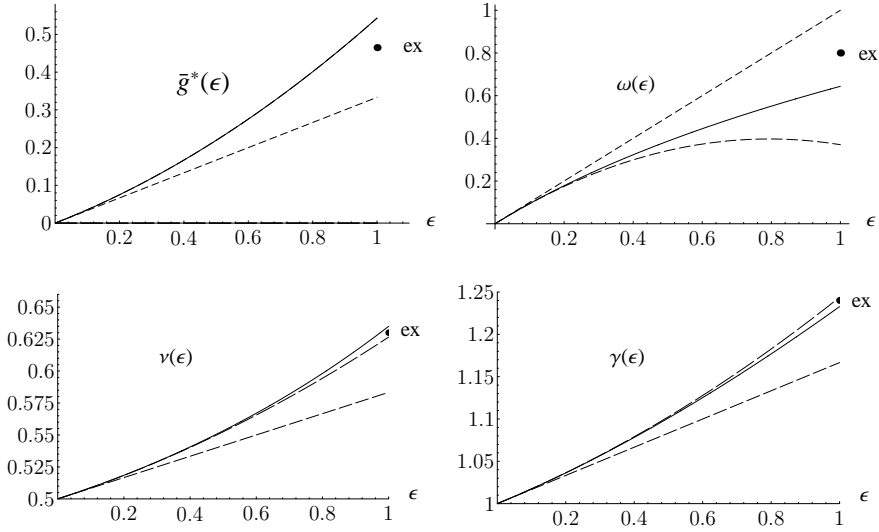


Figure 6: Strong-coupling values of the renormalization group functions for  $n = 1$  (the so-called Ising universality class).

and for the anomalous dimension from Eq. (19), (24), and (25):

$$\eta(g_0) = \frac{n+2}{18}g_0^2 - \frac{(n+2)(n+8)}{216}\left(1 - \frac{8}{\epsilon}\right)g_0^2 + \dots \quad (30)$$

Due to the anomalous dimension  $\eta \neq 0$ , the dependence of the approximations on the variational parameter develops no longer a horizontal flat valley (see Appendix A). Instead, the valley turns out to have a slope which can only be removed by introducing another parameter  $q$  in to substitution rule (7). We rewrite the series in  $g$  as a series in  $g/\kappa^q$ , and replace  $\kappa$  by

$$\kappa \rightarrow \sqrt{K^2 + (\kappa^2 - K^2)} \equiv \sqrt{K^2 + gr}, \quad (31)$$

by

$$r = (\kappa^2 - K^2)/g. \quad (32)$$

As before we re-expand the partial sums of the series in powers of  $g$  at fixed  $r$  up to power  $g^N$  to obtain  $W^N$ . After this we set  $\kappa \rightarrow 1$  and plot  $W^N$  as a function of  $K$ . By varying  $q$  we can make the valley of minimal  $K$ -dependence horizontal [16].

The asymptotic behavior of the variational parameter  $K(g_0)$  and the critical exponent as a function of  $g_0$ , called generically  $f(g_0)$ , is now in general

$$\begin{aligned} K(g_0) &= g^{1/q} \{c_0 + c_1 g_0^{-2/q} + c_2 g_0^{-4/q} + \dots\} \\ f(g_0) &= g^{p/q} \{b_0 + b_1 g_0^{-2/q} + b_2 g_0^{-4/q} + \dots\}, \end{aligned} \quad (33)$$

In the proof of the exponentially fast convergence in Refs. [13, 14, 15]. it was shown that the approach of the correct result proceeds as a function of the highest order  $L$  of the partial sum as  $e^{-cL^{1-2/q}}$ .

In this way we find from (28) the strong-coupling behavior [20]

$$g(g_0) = g^* + b_1 g_0^{-\frac{\omega}{\epsilon}} + \dots, \quad (34)$$

The exponent  $\omega$  is the famous Wegner exponent [21]. Further we find from (29)

$$\frac{m^2(g_0)}{m_0^2} = b_0 g_0^{-\frac{2}{\epsilon}\gamma_m^*} + \dots, \quad (35)$$

where the parameter  $\omega$  and  $\gamma_m^*$  are found from the strong-coupling limits

$$\frac{\omega}{\epsilon} = -1 - g_0 \left[ \frac{g''(g_0)}{g'(g_0)} \right]_{g_0 \rightarrow \infty}, \quad \gamma_m^* = -\frac{\epsilon}{2} \left[ \frac{d \ln m^2(g_0)/m_0^2}{d \ln g_0} \right]_{g_0 \rightarrow \infty}. \quad (36)$$

This parameter determines also the divergence of the coherence length in the critical behavior  $\xi(T) \sim (T - T_c)^{-\nu}$ :

$$\nu = 1/(2 - \gamma_m^*). \quad (37)$$

The results are

$$\omega = \frac{\epsilon}{2 \sqrt{1 + \frac{3(3n+14)\epsilon}{(n+8)^2}} - 1}, \quad \nu = \frac{1 + \frac{5}{2(n+8)}\epsilon}{2 \left[ 1 - \frac{n-3}{2(n+8)}\epsilon - \frac{3(n+2)(3n+14)}{2(n+8)^3}\epsilon^2 \right]}. \quad (38)$$

They are plotted in Fig. 6 as a function of  $\epsilon$ .

Instead of an expansion in  $D = 4 - \epsilon$  dimensions one may also treat expansions obtained by Nickel [22] directly in  $D = 3$  dimensions.

### 3.2. Three-Dimensional Treatment

If one plots the strong-coupling limits of the series obtained from the partial sums of order  $L$  as a function of  $x(L) = e^{-cL^{1-\omega}}$  to account for the theoretical approach to the asymptotic limit, one finds for various  $n$  [23]:

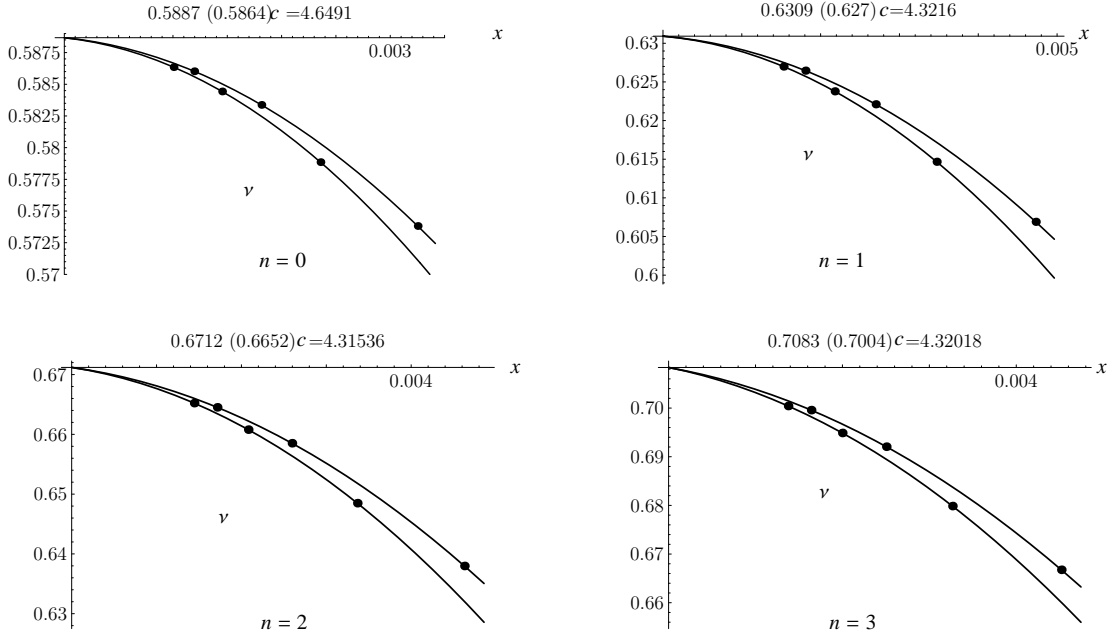


Figure 7: Strong-coupling values for the critical exponent  $\nu^{-1}(x)$  as a function of  $x(L) = e^{-cL^{1-\omega}}$

For the critical exponent  $\alpha$  characterizing the behavior of the specific heat  $C \approx |T - T_c|^{-\alpha}$  of superfluid helium near the critical temperature  $T_c$ , the strong-coupling limit is [15].

$$\alpha \approx 2 - 3 \times 0.6712 \approx -0.0136. \quad (39)$$

If we extrapolate the asymptotic behavior expansion coefficients of  $\nu$  up to the 9th order according using the theoretically known large-order behavior this result can be improved to  $\alpha \approx -0.0129$  [24] (see Fig. 8). This value agrees perfectly with the space shuttle value [8]  $\alpha = -0.01285 \pm 0.00038$ . The experimental result extracted from Fig. 1 and the various theoretical numbers obtained from the divergent perturbation series for  $\alpha$  are summarized in Fig. 9.

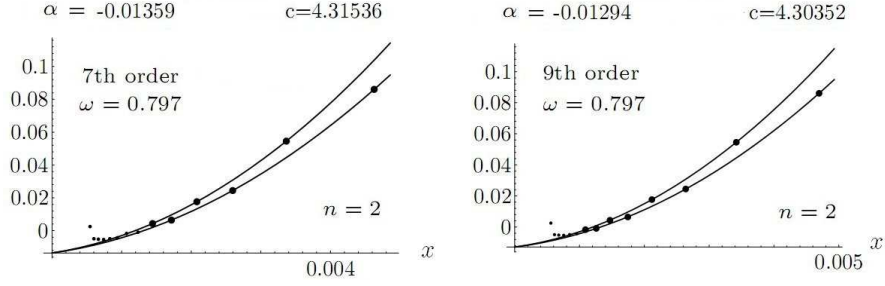


Figure 8: Strong-coupling limits of  $\alpha$  as a function of  $x = e^{-cL^{1-\omega}}$  for 7th and 9th order in perturbation theory. The latter limit  $\alpha \approx -0.0129$  agrees well with the satellite experiment [8].

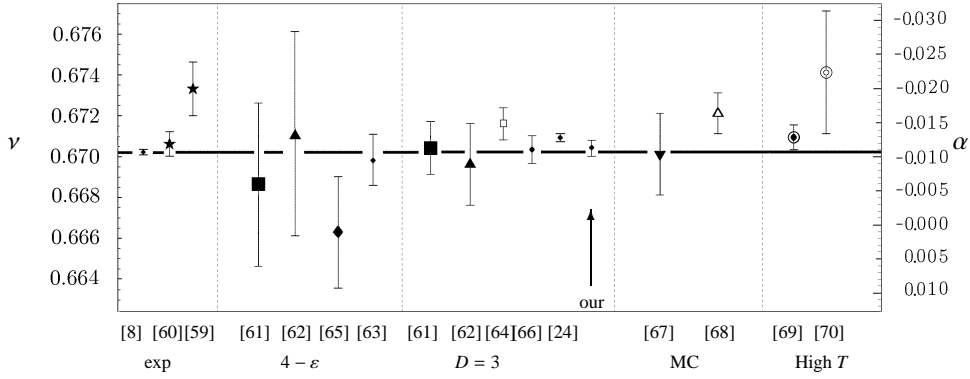


Figure 9: Survey of experimental and theoretical values for  $\alpha$ . The latter come from resummed perturbation expansions of  $\phi^4$ -theory in  $4 - \epsilon$  dimensions, in three dimensions, and from high-temperature expansions of XY-models on a lattice. The sources are indicated below.

#### 4. Shift of the Critical Temperature in Bose-Einstein Condensate by Repulsive Interaction

A free Bose gas condenses at a critical temperature

$$T_c^{(0)} = \frac{2\pi}{M} \left[ \frac{n}{\zeta(3/2)} \right]^{\frac{2}{3}}, \quad (40)$$

where  $n$  is the particle density. A small relative shift of  $T_c$  with respect to  $T_c^{(0)}$  can be calculated from the general formula

$$\frac{\Delta T_c}{T_c^{(0)}} = -\frac{2}{3} \frac{\Delta n}{n^{(0)}}, \quad (41)$$

where  $n^{(0)}$  is the particle density in the free condensate and  $\Delta n$  its change at  $T_c$  caused by a small repulsive point interaction parametrized by an  $s$ -wave scattering length  $a$ . For small  $a$ , this behaves like [25, 26]

$$\frac{\Delta T_c}{T_c^{(0)}} = c_1 a n^{1/3} + [c'_2 \ln(a n^{1/3}) + c_2] a^2 n^{2/3} + O(a^3 n). \quad (42)$$

where  $c'_2 = -64\pi\zeta(1/2)/3\zeta(3/2)^{5/3} \simeq 19.7518$  can be calculated perturbatively, whereas  $c_1$  and  $c_2$  require non-perturbative techniques since infrared divergences at  $T_c$  make them basically strong-coupling results. The standard technique to reach this regime is based on a resummation of perturbation expansions using the renormalization group [27, 18], first applied in this context by Ref. [28].



Using quantum field theory, the temperature shift can be found from the formula

$$\frac{\Delta T_c}{T_c^{(0)}} \approx -\frac{2}{3} \frac{MT_c^{(0)}}{n} \langle \Delta \phi^2 \rangle = -\frac{4\pi}{3} \frac{(MT_c^{(0)})^2}{n} 4! \left\langle \frac{\Delta \phi^2}{u} \right\rangle a = -\frac{4\pi}{3} (2\pi)^2 \frac{1}{[\zeta(3/2)]^{4/3}} 4! \left\langle \frac{\Delta \phi^2}{u} \right\rangle a n^{1/3}, \quad (43)$$

corresponding in Eq. (42) to

$$c_1 \approx -1103.09 \left\langle \frac{\Delta \phi^2}{u} \right\rangle. \quad (44)$$

A calculation of the Feynman diagrams in Fig. 10 yields the following five-loop perturbation expansion for the expectation value  $\langle \phi^2/u \rangle$  [29, 30]

$$\begin{aligned} \left\langle \frac{\phi^2}{u} \right\rangle &= F(u) \equiv -\frac{N}{4\pi} \frac{m}{u} - a_2 \frac{N(2+N)}{18(4\pi)^3} \frac{u}{m} + a_3 \frac{N(16+10N+N^2)}{108(4\pi)^5} \left(\frac{u}{m}\right)^2 \\ &\quad - \left[ a_{41} \frac{N(2+N)^2}{324(4\pi)^7} + a_{42} \frac{N(40+32N+8N^2+N^3)}{648(4\pi)^7} + a_{43} \frac{N(44+32N+5N^2)}{324(4\pi)^7} \right. \\ &\quad \left. + a_{44} \frac{N(2+N)^2}{324(4\pi)^7} + a_{45} \frac{N(44+32N+5N^2)u^4}{324m^3(4\pi)^7} \right] \left(\frac{u}{m}\right)^3 + \dots \end{aligned} \quad (45)$$

where  $a_2 \equiv \log(4/3)/2 \approx 0.143841$  and the other constants are only known numerically [31]:

$$a_3 = 0.642144, \quad a_{41} = -0.115069, \quad a_{42} = 3.128107, \quad a_{43} = 1.63, \quad a_{44} = -0.624638, \quad a_{45} = 2.39. \quad (46)$$

Writing the above expansion up to the  $L$ th term as  $F_L(u) = \sum_{l=-1}^L f_l (u/4\pi m)^l$ , the expansion coefficients for the relevant number of components  $N = 2$  are [31]:

$$f_{-1} = -126.651 \times 10^{-4}, \quad f_0 = 0, \quad f_1 = -4.04837 \times 10^{-4}, \quad f_2 = 2.39701 \times 10^{-4}, \quad f_3 = -1.80 \times 10^{-4}. \quad (47)$$

We need the value of the series  $F_L(u)$  in the critical limit  $m \rightarrow 0$ , which is obviously equivalent to the strong-coupling limit of  $F_L(u)$ . As mentioned above, this limit should be most accurately found with the help of variational perturbation theory [32, 33, 18].

If the series were of quantum mechanical origin, we could have found this limit by applying the square-root trick (7) of Ref. [6]. In the present situation where we are only interested in the extreme strong-coupling limit, we would form the sequence of truncated expansions  $F_L(u)$  for 1, 2, 3 and replace each term

$$(u/m)^l \rightarrow K^l [1 - 1]_{L-l}^{-l/2} \quad (48)$$

where the symbol  $[1 - 1]_k^r$  is defined as the binomial expansion of  $(1 - 1)^r$  truncated after the  $k$ th term

$$[1 - 1]_k^r \equiv \sum_{i=0}^k \binom{r}{i} (-1)^i = (-1)^k \binom{r-1}{k}. \quad (49)$$

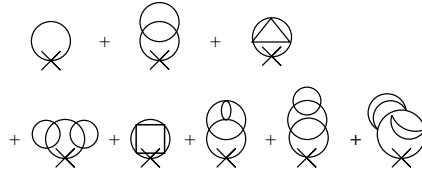


Figure 10: Diagrams contributing to the expectation value  $\langle \phi^2 \rangle$ .

Table 1: Trial functions for the naive quantum-mechanical variational perturbation expansion

$$\begin{aligned} W_1^{\text{QM}} &= -0.0596831 K^{-1} - 0.0000322159 K, \\ W_2^{\text{QM}} &= -0.0497359 K^{-1} - 0.0000483239 K + 1.51792 \cdot 10^{-6} K^2, \\ W_3^{\text{QM}} &= -0.0435189 K^{-1} - 0.0000604049 K + 3.03584 \cdot 10^{-6} K^2 - .908 \cdot 10^{-7} K^3. \end{aligned}$$

The resulting expressions must be optimized in the variational parameter  $K$ . They are listed in Table 1. The approximants  $W_{1,2,3}^{\text{QM}}$  have extrema  $W_{1,2,3}^{\text{QMext}} \approx -0.00277, +0.00405, -0.0029$ , corresponding, via (44), to  $c_1 \approx 3.059, -4.46, 3.01$ . These values have previously been obtained in Ref. [29] in a much more complicated way via a so-called  $\delta$ -expansion. Note the negative sign of the second approximation arising from the fact that an extremum exists only at negative  $K$ . According to our rules of variational perturbation theory one should, in this case, use the saddle point at positive  $K$  which would yield  $W_2^{\text{QM}} = -0.00153$  corresponding to  $c_1 \approx 1.69$  rather than -4.46, leading to the more reasonable approximation sequence  $c_1 \approx 3.059, 1.69, 3.01$ , which shows no sign of convergence. In  $W_3^{\text{QM}}$ , there is also a pair of complex extrema from which the authors of Ref. [29] extract the real part  $\text{Re } \tilde{W}_{3\text{complex}}^{\text{QM}} \approx -0.00134$  corresponding to  $c_1 \approx 1.48$ , which they state as their final result. There is, however, no acceptable theoretical justification for such a choice [16].

This lack of convergence is not astonishing since we are dealing with field theory, where the dimensions are anomalous and the naive principle of minimal sensitivity breaks down (contrary to ubiquitous statements in the literature [34]). The valley in the dependence on the variational parameter is no longer horizontal [16].

The correct procedure goes as follows: We form the logarithmic derivative of the expansion (45):

$$\beta(u) \equiv \frac{\partial \log F(u)}{\partial \log u} = -1 + 2 \frac{f_1}{f_{-1}} \left(\frac{u}{m}\right)^2 + 3 \frac{f_2}{f_{-1}} \left(\frac{u}{m}\right)^3 + \left(4 \frac{f_3}{f_{-1}} - 2 \frac{f_1^2}{f_{-1}^2}\right) \left(\frac{u}{m}\right)^4 + \dots \quad (50)$$

In order for  $F(u)$  to go to a constant in the critical limit  $m \rightarrow 0$ , this function must go to zero in the strong-coupling limit  $u \rightarrow \infty$ . Writing the expansion as  $\beta_L(u) = -1 + \sum_{l=2}^L b_l (u/4\pi m)^l$ , the coefficients are

$$b_2 = 0.0639293, \quad b_3 = -0.056778, \quad b_4 = 0.0548799. \quad (51)$$

The sums  $\beta_L(u)$  have to be evaluated for  $u \rightarrow \infty$  allowing for the universal anomalous dimension  $\omega$  by which the physical observables of  $\phi^4$ -theories approach the scaling limit [27, 18]. The approach to the critical point  $A + B(m/u)^{\omega'}$  where  $\omega' = \omega/(1 - \eta/2)$  [35]. The exponent  $\eta$  is the small anomalous dimension of the field while  $\omega$  again the Wegner exponent [21] of renormalization group theory  $\Delta \equiv \omega\nu$ . Here it appears in the variational expression for the strong-coupling limit which is found [32, 33] by replacing  $(u/m)^l$  by  $K^l [1 - 1]_{L-l}^{-q/2}$ , where  $q \equiv 2/\omega'$ . Thus we obtain the variational expressions

$$W_3^\beta = -1 + \left(\frac{2f_1}{f_{-1}} + \frac{2f_1 q}{f_{-1}}\right) K^2 + \frac{3f_2}{f_{-1}} K^3 \quad (52)$$

$$W_4^\beta = -1 + \left(\frac{2f_1}{f_{-1}} + \frac{3f_1 q}{f_{-1}} + \frac{f_1 q^2}{f_{-1}}\right) K^2 + \left(\frac{3f_2}{f_{-1}} + \frac{9f_2 q}{2f_{-1}}\right) K^3 + \left(\frac{-2f_1^2}{f_{-1}^2} + \frac{4f_3}{f_{-1}}\right) K^4 \quad (53)$$

The first has a vanishing extremum at  $\omega'_3 = 0.592$ , the second has neither an extremum nor a saddle point. However, a complex pair of extrema lies reasonably close to the real axis at  $\omega'_4 = 0.635 \pm 0.116$ , whose real part is not far from the true exponent of approach  $\omega'_\infty \approx 0.81$  [27, 18], to which  $\omega'_L$  will converge for order  $L \rightarrow \infty$  [32]. Given these  $\omega'$ -values, we now form the variational expressions  $W_L$  from  $F_L$  by the replacement  $(u/m)^l \rightarrow K^l [1 - 1]_{L-l}^{-q/2}$ , which are

$$W_2 = f_{-1} \left(1 - \frac{3}{4}q + \frac{1}{8}q^2\right) K^{-1} + f_1 K, \quad (54)$$

$$W_3 = f_{-1} \left(1 - \frac{11}{13}q + \frac{1}{4}q^2 - \frac{1}{48}q^3\right) K^{-1} + f_1 \left(1 + \frac{q}{2}\right) K + f_2 K^2, \quad (55)$$

$$W_4 = f_{-1} \left(1 - \frac{25}{24}q + \frac{35}{96}q^2 - \frac{5}{96}q^3 + \frac{1}{384}q^4\right) K^{-1} + f_1 \left(1 + \frac{3}{4}q + \frac{1}{8}q^2\right) K + f_2 (1 + q) K^2 + f_3 K^3. \quad (56)$$

The lowest function  $W_2$  is optimized with the naive growth parameter  $q = 1$  since to this order no anomalous value can be determined from the zero of the beta function (50). The optimal result is  $W_2^{\text{opt}} = -\sqrt{\log[4/3]/6}/8\pi^2 \approx -0.00277$  corresponding to  $c_1 \equiv 3.06$ . The next function  $W_3$  is optimized with the above determined  $q_3 = 2/\omega'_3$  and yields  $W_3^{\text{opt}} \approx -0.000976$  corresponding to  $c_1 \equiv 1.078$ . Although  $\omega'_4$  is not real we shall insert its real part into  $W_4$  and find  $W_4^{\text{opt}} \equiv -0.000957$  corresponding to  $c_1 \equiv 1.057$ . The three values of  $c_1$  for  $\bar{L} \equiv L - 1 = 1, 2, 3$  can well be fitted by a function  $c_1 \approx 1.053 + 2/\bar{L}^6$  (see Fig. 11). Such a fit is suggested by the general large- $L$  behavior  $a + be^{-c\bar{L}^{1-\omega'}}$  which was derived in Refs. [6]. Due to the smallness of  $1 - \omega' \approx 0.2$ , this can be replaced by  $\approx a' + b'/\bar{L}^s$ .

Alternatively, we may optimize the functions  $W_{1,2,3}$  using the known precise value of  $q_\infty = 2/\omega'_\infty \approx 2/0.81$ . Then  $W_2$  turns out to have no optimum, whereas the others yield  $W_{3,4}^{\text{opt}} \approx -0.000554, -0.000735$ , corresponding via Eq. (44) to  $c_1 = 0.580, 0.773$ . If these two values are fitted by the same inverse power of  $\bar{L}$ , we find  $c_1 \approx 0.83 - 14/\bar{L}^6$ . From the extrapolations to infinite order we estimate  $c_{1,\infty} \approx 0.92 \pm 0.13$ .

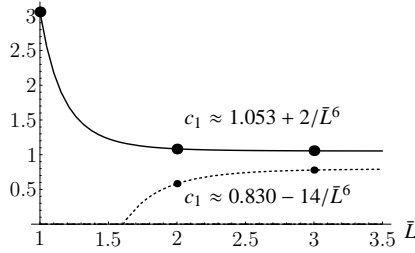


Figure 11: The three approximants for  $c_1$  plotted against the order of variational approximation  $\bar{L} \equiv L - 1 = 1, 2, 3$ , and extrapolation to the infinite-order limit.

This result is to be compared with latest Monte Carlo data which estimate  $c_1 \approx 1.32 \pm 0.02$  [36, 37]. Previous theoretical estimates are  $c_1 \approx 2.90$  [38], 2.33 from a  $1/N$ -expansion [39]), 1.71 from a next-to-leading order in a  $1/N$ -expansion [40], 3.059 from an inapplicable  $\delta$ -expansion [41] to three loops, and 1.48 from the same  $\delta$ -expansion to five loops, with a questionable evaluation at a complex extremum [29] and some wrong expansion coefficients (see [31]). Remarkably, our result lies close to the average between the latest and the first Monte Carlo result  $c_1 \approx 0.34 \pm 0.03$  in Ref. [42].

As a cross check of the reliability of our theory consider the result in the limit  $N \rightarrow \infty$ . Here we must drop the first term in the expansion (45) which vanishes at the critical point (but would diverge for  $N \rightarrow \infty$  at finite  $m$ ). The remaining expansion coefficients of  $\langle \phi^2/u \rangle/N$  in powers of  $Nu/4\pi m$  are

$$f_1 = -6.35917 \cdot 10^{-4}, \quad f_2 = 4.7315 \cdot 10^{-4}, \quad f_3 = -3.84146 \cdot 10^{-4}. \quad (57)$$

Using the  $N \rightarrow \infty$  limit of  $\omega'$  which is equal to 1 implying  $q = 2$  in Eqs. (55) and (56), we obtain the two variational approximations

$$W_2^\infty = -0.00127183K + 0.00047315K^2, \quad W_3^\infty = -0.00190775K + 0.00141945K^2 - 0.000384146K^3, \quad (58)$$

whose optima yield the approximations  $c_1 \approx 1.886$  and  $2.017$ , converging rapidly towards the exact large- $N$  result 2.33 of Ref. [39], with a 10% error.

Numerically, the first two  $1/N$ -corrections found from a fit to large- $N$  results obtained by using the known large- $N$  expression for  $\omega' = 1 - 8(8/3\pi^2 N) + 2(104/3 - 9\pi^2/2)(8/3\pi^2 N)^2$  [43] produce a finite- $N$  correction factor  $(1 - 3.1/N + 30.3/N^2 + \dots)$ , to be compared with  $(1 - 0.527/N + \dots)$  obtained in Ref. [40].

Since the large- $N$  results can only be obtained so well without the use of the first term we repeat the evaluations of the series at the physical value  $N = 2$  without the first term, where the variational expressions for  $f$  are

$$\begin{aligned} W_2 &= f_1 \left(1 + \frac{q}{2}\right) K + f_2 K^2, \\ W_3 &= f_1 \left(1 + \frac{3}{4}q + \frac{1}{8}q^2\right) K + f_2 (1 + q) K^2 + f_3 K^3. \end{aligned} \quad (59)$$

The lowest order optimum lies now at  $W_2^{\text{opt}} = -f_1^2(2+q)^2/16f_2^2$ , yielding  $c_1 \equiv 0.942$  for the exact  $q = 2/0.81$ . To next order, an optimal turning point of  $W_3$  yields  $c_1 \approx 1.038$ .

At this order, we can derive a variational expression for the determination of  $\omega'$  using the analog of Eq. (50) which reads

$$\beta(u) \equiv \frac{\partial \log F(u)}{\partial \log u} = 1 + \frac{f_2}{f_1} \frac{u}{m} + \left(2 \frac{f_3}{f_1} - \frac{f_2^2}{f_1^2}\right) \left(\frac{u}{m}\right)^2 + \dots \quad (60)$$

After the replacement (48) we find

$$W_3^\beta = 1 + \frac{f_2(1+q/2)}{f_1} K + \left(2 \frac{f_3}{f_1} - \frac{f_2^2}{f_1^2}\right) K^2 + \dots \quad (61)$$

whose vanishing extremum determines  $\omega' = 2/q$  as being

$$\omega'_3 = \left(2 \sqrt{2f_1 f_3 / f_2^2} - 1 - 1\right)^{-1} \approx 0.675, \quad (62)$$

leading to  $c_1 \approx 1.238$  from an optimal turning point of  $W_3$ . There are now too few points to perform an extrapolation to infinite order. From the average of the two highest-order results we obtain our final estimate:  $c_1 \approx 1.14 \pm 0.11$ , such that the critical temperature shift is

$$\frac{\Delta T_c}{T_c^{(0)}} \approx (1.14 \pm 0.11) a n^{1/3}. \quad (63)$$

This lies reasonably close to the Monte Carlo number  $c_1 \approx 1.32 \pm 0.02$ .

## 5. Membrane Between Walls

As another example consider a tension-free membrane of bending stiffness  $\kappa$  between hard walls [44] (see Fig. 12).

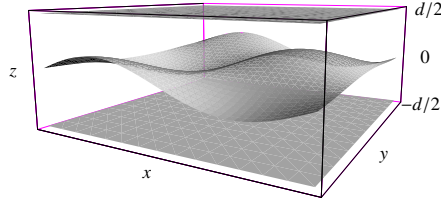


Figure 12: Membrane fluctuating between walls with distance  $d$ .

Its thermal fluctuations are described by a functional integral over a Boltzmann factor

$$Z = \prod_x \int_{-d/2}^{d/2} \mathcal{D}h e^{-E/k_0 T}, \quad (64)$$

where  $h(x)$  is the height function of the membrane and  $E$  is the bending energy

$$E = \frac{\kappa}{2} \int d^2 x \left[ \partial^2 h(x) \right]^2. \quad (65)$$

This functional integral has not been solved exactly, in spite of its simplicity. It can, however, be approximated by the functional integral

$$Z = \prod_x \int_{-\infty}^{\infty} \mathcal{D}h e^{-[E+V(x)]/k_0 T}, \quad (66)$$

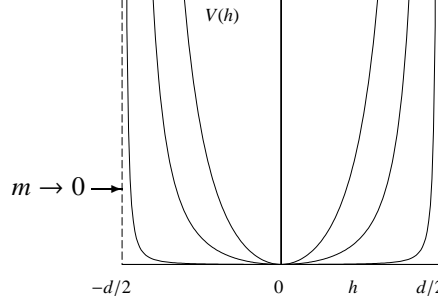


Figure 13: Softened hard-wall potential which becomes infinitely hard in the limit  $m \rightarrow 0$

in which the height fluctuates between  $-\infty$  and  $\infty$  in a potential (see Fig. 13)

$$V(x) = m^4 \frac{d^2}{\pi^2} \tan^2\left(\frac{\pi h}{d}\right). \quad (67)$$

This problem can be solved perturbatively yielding  $Z = e^{-Af}$ , where  $A$  is the area of the membrane and  $f$  has, to order  $N$ , the series

$$f^N = \frac{m^2}{2} \left[ 1 + \frac{1}{8} + \frac{\pi^2}{m^2 d^2} \frac{1}{64} + \dots + \left( \frac{\pi^2}{m^2 d^2} \right)^N a_N \dots \right]. \quad (68)$$

The hard-wall limit  $m \rightarrow 0$  amounts to the strong-coupling limit of this series.

We expand the potential (4) into a power series

$$V(h) = m^4 \frac{h^2}{2} + m^4 \frac{\pi^2}{d^2} \left\{ \frac{1}{3} h^4 + \frac{17}{90} \frac{\pi^2}{d^2} h^6 + \frac{31}{315} \frac{\pi^4}{d^4} h^8 + \frac{691}{14175} \frac{\pi^6}{d^6} h^{12} + \frac{10922}{467775} \frac{\pi^8}{d^8} h^{16} + \dots \right\}. \quad (69)$$

If we denote the interaction terms by

$$V^{\text{int}} = \frac{\kappa m^4}{2} \sum_{k=1}^{\infty} \varepsilon_k \left( \frac{\pi}{d} h \right)^{2k}, \quad (70)$$

and calculate the Feynman diagrams shown in Fig. 14, The functional integral (64) can be expressed as an exponential

$$\begin{aligned} F^4 = & \frac{1}{2} \bigcirc + 3 \infty + 15 \text{ (figure-eight)} + \frac{1}{2} (72 \text{ (two loops)} + 24 \text{ (figure-eight with cross)}) \\ & + 105 \text{ (four loops)} + \frac{1}{2} (540 \text{ (three loops)} + 360 \text{ (figure-eight with cross)}) \\ & + \frac{1}{6} \left( 1728 \text{ (four loops)} + 3456 \text{ (figure-eight with cross)} + 1728 \text{ (three loops)} + 2592 \text{ (four loops)} \right) \end{aligned}$$

Figure 14: Feynman diagrams in the perturbative expansion of the free energy of the Membrane between walls up to the order  $N = 4$ .

$Z = e^{-Af}$ , where  $A$  is the area of the membrane and

$$f^N = \frac{m^2}{2} \left[ 1 + \frac{1}{8} + \frac{\pi^2}{m^2 d^2} \frac{1}{64} + \dots + \left( \frac{\pi^2}{m^2 d^2} \right)^N a_N \dots \right]. \quad (71)$$

Using the Bender-Wu recursion relations [46], we can express the coefficients in terms of  $\varepsilon_K$  as

$$\begin{aligned} f^N = & \frac{m^2}{2} + \frac{3\pi^2}{4d^2} \varepsilon_4 - \frac{\pi^4}{8d^4} (21\varepsilon_4^2 - 15\varepsilon_6) + \frac{\pi^6}{16d^6} (333\varepsilon_4^3 - 360\varepsilon_4\varepsilon_6 + 105\varepsilon_8) \\ & - \frac{\pi^8}{128d^8} (30885\varepsilon_4^4 - 44880\varepsilon_4^2\varepsilon_6 + 6990\varepsilon_6^2 + 1512\varepsilon_4\varepsilon_8 + 3780\varepsilon_{10}) + \dots \end{aligned}$$

The hard-wall result is obtained in the limit  $m \rightarrow 0$ , which is the strong-coupling limit of the series (71).

## 6. Variational Perturbation Theory of Tunneling

None of the presently known resummation schemes [19, 18] is able to deal with non-Borel-summable series. Such series arise in the theoretical description of many important physical phenomena, in particular tunneling processes. In the path integral, these are dominated by non-perturbative contributions coming from nontrivial classical solutions called *critical bubbles* [45, 6] or *bounces* [47], and fluctuations around these.

A non-Borel-summable series can become Borel-summable if the expansion parameter, usually some coupling constant  $g$ , is continued to negative values. In this way, non-Borel-summable series can be evaluated with any desired accuracy by an analytic continuation of variational perturbation theory [6, 18] in the complex  $g$ -plane. This implies that variational perturbation theory can give us information on non-perturbative properties of the theory.

### 6.1. Test of Variational Perturbation Theory for Simple Model of Non-Borel-summable Expansions

The partition function  $Z(g)$  of the anharmonic oscillator in zero space-time dimensions is

$$Z(g) = \frac{1}{\sqrt{\pi}} \int_{-\infty}^{\infty} \exp(-x^2/2 - g x^4/4) dx = \frac{\exp(1/8g)}{\sqrt{4\pi g}} K_{1/4}(1/8g), \quad (72)$$

where  $K_\nu(z)$  is the modified Bessel function. For small  $g$ , the function  $Z(g)$  has a divergent Taylor series expansion, to be called *weak-coupling expansion*:

$$Z_{\text{weak}}^{(L)}(g) = \sum_{l=0}^L a_l g^l, \quad \text{with } a_l = (-1)^l \frac{\Gamma(2l + 1/2)}{l! \sqrt{\pi}}. \quad (73)$$

For  $g < 0$ , this is non-Borel-summable. For large  $|g|$  there exists a convergent *strong-coupling expansion*:

$$Z_{\text{strong}}^{(L)}(g) = g^{-1/4} \sum_{l=0}^L b_l g^{-l/2}, \quad \text{with } b_l = (-1)^l \frac{\Gamma(l/2 + 1/4)}{2l! \sqrt{\pi}}. \quad (74)$$

As is obvious from the integral representation (72),  $Z(g)$  obeys the second-order differential equation

$$16g^2 Z''(g) + 4(1 + 8g)Z'(g) + 3Z(g) = 0, \quad (75)$$

which has two independent solutions. One of them is  $Z(g)$ , which is finite for  $g > 0$  with  $Z(0) = a_0$ . The weak-coupling coefficients  $a_l$  in (73) can be obtained by inserting into (75) the Taylor series and comparing coefficients. The result is the recursion relation

$$a_{l+1} = -\frac{16l(l+1)+3}{4(l+1)} a_l. \quad (76)$$

A similar recursion relation can be derived for the strong-coupling coefficients  $b_l$  in Eq. (74). We observe that the two independent solutions  $Z(g)$  of (75) behave like  $Z(g) \propto g^\alpha$  for  $g \rightarrow \infty$  with the powers  $\alpha = -1/4$  and  $-3/4$ . The function (72) has  $\alpha = -1/4$ . It is convenient to remove the leading power from  $Z(g)$  and define a function  $\zeta(x)$  such that  $Z(g) = g^{-1/4} \zeta(g^{-1/2})$ . The Taylor coefficients of  $\zeta(x)$  are the strong-coupling coefficients  $b_l$  in Eq. (74). The function  $\zeta(x)$  satisfies the differential equation and initial conditions:

$$4\zeta''(x) - 2x\zeta'(x) - \zeta(x) = 0, \quad \text{with } \zeta(0) = b_0 \text{ and } \zeta'(0) = b_1. \quad (77)$$

The Taylor coefficients  $b_l$  of  $\zeta(x)$  satisfy the recursion relation

$$b_{l+2} = \frac{2l+1}{4(l+1)(l+2)} b_l. \quad (78)$$

Analytic continuation of  $Z(g)$  around  $g = \infty$  to the left-hand cut gives:

$$Z(-g) = (-g)^{-1/4} \zeta((-g)^{-1/2}) \quad (79)$$

$$= (-g)^{-1/4} \sum_{l=0}^{\infty} b_l (-g)^{-l/2} \exp\left[-\frac{i\pi}{4}(2l+1)\right] \quad \text{for } g > 0, \quad (80)$$

so that we find an imaginary part

$$\text{Im } Z(-g) = -(4g)^{-1/4} \sum_{l=0}^{\infty} b_l (-g)^{-l/2} \sin\left[-\frac{i\pi}{4}(2l+1)\right] \quad (81)$$

$$= -(4g)^{-1/4} \sum_{l=0}^{\infty} \beta_l (-g)^{-l/2}, \quad (82)$$

where

$$\beta_0 = b_0, \quad \beta_1 = b_1, \quad \beta_{l+2} = -\frac{2l+1}{4(l+1)(l+2)} \beta_l. \quad (83)$$

It is easy to show that

$$\sum_{l=0}^{\infty} \beta_l x^l = \zeta(x) \exp(-x^2/4), \quad (84)$$

so that

$$\text{Im } Z(-g) = -\frac{1}{\sqrt{2}} g^{-1/4} \exp(-1/4g) \sum_{l=0}^{\infty} b_l g^{-l/2}. \quad (85)$$

From this we may re-obtain the weak-coupling coefficients  $a_l$  by means of the dispersion relation

$$Z(g) = -\frac{1}{\pi} \int_0^{\infty} \frac{\text{Im } Z(-z)}{z+g} dz \quad (86)$$

$$= \frac{1}{\pi \sqrt{2}} \sum_{j=0}^{\infty} b_j \int_0^{\infty} \frac{\exp(-1/4z) z^{-j/2-1/4}}{z+g} dz. \quad (87)$$

Indeed, replacing  $1/(z+g)$  by  $\int_0^{\infty} \exp(-x(z+g)) dx$ , and expanding  $\exp(-xg)$  into a power series, all integrals can be evaluated to yield:

$$Z(g) = \frac{1}{\pi} \sum_{j=0}^{\infty} 2^j b_j \sum_{l=0}^{\infty} (-g)^l \Gamma(l+j/2+1/4). \quad (88)$$

Thus we find for the weak-coupling coefficients  $a_l$  an expansion in terms of the strong-coupling coefficients

$$a_l = \frac{(-1)^l}{\pi} \sum_{j=0}^{\infty} 2^j b_j \Gamma(l+j/2+1/4). \quad (89)$$

Inserting  $b_j$  from Eq. (74), this becomes

$$a_l = \frac{(-1)^l}{2\pi^{3/2}} \sum_{j=0}^{\infty} \frac{2^j (-1)^j}{j!} \Gamma(j/2+1/4) \Gamma(l+j/2+1/4) = (-1)^l \frac{\Gamma(2l+1/2)}{l! \sqrt{\pi}}, \quad (90)$$

coinciding with (73).

Let us now apply variational perturbation theory to the weak-coupling expansion (73). We have seen in Eq. (79), that the strong-coupling expansion can easily be continued analytically to negative  $g$ . This continuation can, however, be used for an evaluation only for sufficiently large  $|g|$  where the strong-coupling expansion converges. In the tunneling regime near the tip of the left-hand cut, the expansion diverges. Let us show that an evaluation of the weak-coupling expansion according to the rules of variational perturbation theory continued into the complex plane gives extremely good results on the entire left-hand cut with a fast convergence even near the tip at  $g = 0$ .

The  $L$ th variational approximation to  $Z(g)$  is given by (see [15, 32, 33, 18])

$$Z_{\text{var}}^{(L)}(g, \Omega) = \Omega^p \sum_{j=0}^L \left( \frac{g}{\Omega^q} \right)^j \epsilon_j(\sigma), \quad (91)$$

with

$$\sigma \equiv \Omega^{q-2}(\Omega^2 - 1)/g, \quad (92)$$

where  $q = 2/\omega = 4$ ,  $p = -1$  and

$$\epsilon_j(\sigma) = \sum_{l=0}^j a_l \binom{(p-lq)/2}{j-l} (-\sigma)^{j-l}. \quad (93)$$

In order to find a valley of minimal sensitivity, the zeros of the derivative of  $Z_{\text{var}}^{(L)}(g, \Omega)$  with respect to  $\Omega$  are needed. They are given by the zeros of the polynomials in  $\sigma$ :

$$P^{(L)}(\sigma) = \sum_{l=0}^L a_l (p - lq + 2l - 2L) \binom{(p-lq)/2}{L-l} (-\sigma)^{L-l} = 0, \quad (94)$$

since it can be shown [13, 15] that the derivative depends only on  $\sigma$ :

$$\frac{dZ_{\text{var}}^{(L)}(g, \Omega)}{d\Omega} = \Omega^{p-1} \left( \frac{g}{\Omega^q} \right)^L P^{(L)}(\sigma). \quad (95)$$

Consider in more detail the lowest non-trivial order with  $L = 1$ . From Eq. (94) we obtain

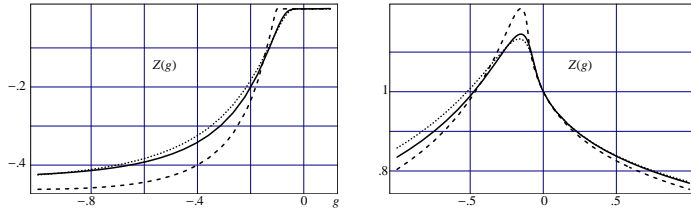


Figure 15: Plot of the 1st- and 2nd-order calculation for the non-Borel-summable region of  $g < 0$ , where the function has a cut with non-vanishing imaginary part: imaginary (left) and real parts (right) of  $Z_{\text{var}}^{(1)}(g)$  (dashed curve) and  $Z_{\text{var}}^{(2)}(g)$  (solid curve) are plotted against  $g$  and compared with the exact values of the partition function (dotted curve). The root of (92) giving the optimal variational parameter  $\Omega$  has been chosen to reproduce the weak-coupling result near  $g = 0$ .

$$\sigma = \frac{5}{2}, \quad \text{corresponding to} \quad \Omega = \frac{1}{2} \left( 1 \pm \sqrt{1 + 10g} \right). \quad (96)$$

In order to ensure that our method reproduces the weak-coupling result for small  $g$ , we have to take the positive sign in front of the square root. In Fig. 15 we have plotted  $Z_{\text{var}}^{(1)}(g)$  (dashed curve) and  $Z_{\text{var}}^{(2)}(g)$  (solid curve) and compared these with the exact result (dotted curve) in the tunneling regime. The agreement is quite good even at these low orders [51]. Next we study the behavior of  $Z_{\text{var}}^{(L)}(g)$  to higher orders  $L$ . For selected coupling values in the non-Borel-summable



region,  $g = -.01, -.1, -1, -10$ , we want to see the error as a function of the order. We want to find from this model system the rule for selecting systematically the best zero of  $P^{(L)}(\sigma)$  solving Eq. (94), which leads to the optimal value of the variational parameter  $\Omega$ . For this purpose we plot the variational results of all zeros. This is shown in Fig. 16, where the logarithm of the deviations from the exact value is plotted against the order  $L$ . The outcome of different zeros cluster strongly near the best value. Therefore, choosing any zero out of the middle of the cluster is reasonable, in particular, because it does not depend on the knowledge of the exact solution, so that this rule may be taken over to realistic cases.

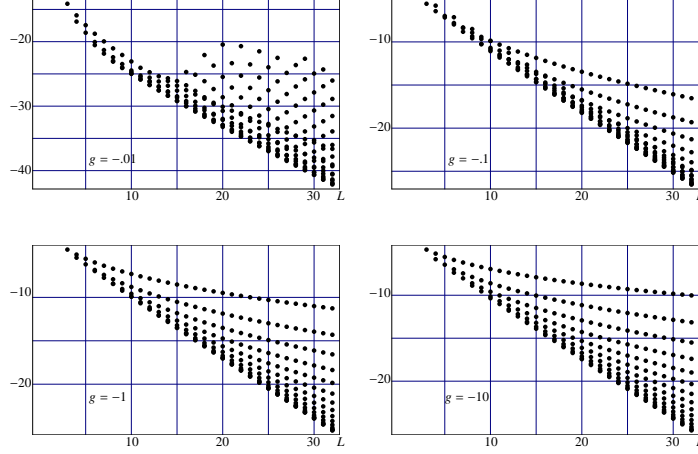


Figure 16: Logarithm of deviation of the variational results from exact values  $\log|Z_{\text{var}}^{(L)} - Z_{\text{exact}}|$  plotted against the order  $L$  for different  $g < 0$  in the non-Borel-summable region. All complex optimal  $\Omega$ 's have been used.

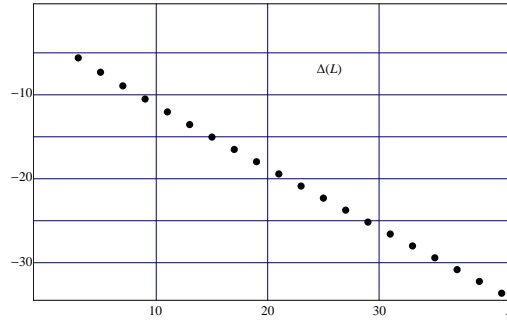


Figure 17: Logarithm of deviation of variational results from exactly known value  $\Delta(L) = \log|Z_{\text{var}}^{(L)} - Z_{\text{exact}}|$ , plotted against the order  $L$  for  $g = 10$  in Borel-summable region. The real positive optimal  $\Omega$  have been used. There is only one real zero of the first derivative in every odd order  $L$  and none for even orders. There is excellent convergence  $\Delta(L) \simeq 0.02 \exp(-0.73L)$  for  $L \rightarrow \infty$ .

We wish to emphasize, that for the Borel-summable domain with  $g > 0$ , variational perturbation theory has the usual fast convergence in this model. In fact, for  $g = 10$ , probing deeply into the strong-coupling domain, we find rapid convergence like  $\Delta(L) \simeq 0.02 \exp(-0.73L)$  for  $L \rightarrow \infty$ , where  $\Delta(L) = \log|Z_{\text{var}}^{(L)} - Z_{\text{exact}}|$  is the logarithmic error as a function of the order  $L$ . This is shown in Fig. 17. Furthermore, the strong-coupling coefficients  $b_l$  of Eq. (74) are reproduced quite satisfactorily. Having solved  $P^{(L)}(\sigma) = 0$  for  $\sigma$ , we obtain  $\Omega^{(L)}(g)$  by solving Eq. (92). Inserting this and (93) into (91), we bring  $g^{1/4} Z_{\text{var}}^{(L)}(g)$  into a form suitable for expansion in powers of  $g^{-1/2}$ . The expansion coefficients are the strong-coupling coefficients  $b_l^{(L)}$  to order  $L$ . In Fig. 18 we have plotted the logarithms of their absolute and relative errors over the order  $L$ , and find very good convergence, showing that variational perturbation

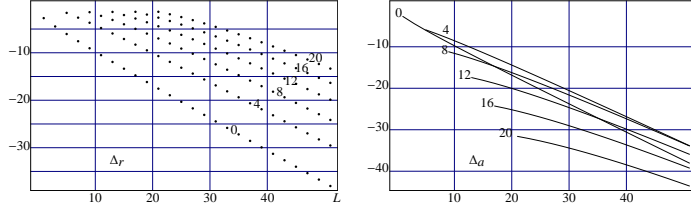


Figure 18: Relative logarithmic error  $\Delta_r = \log |1 - b_l^{(L)}/b_l^{(\text{exact})}|$  on the left, and the absolute logarithmic error  $\Delta_a = \log |b_l^{(L)} - b_l^{(\text{exact})}|$  on the right, plotted for some strong-coupling coefficients  $b_l$  with  $l = 0, 4, 8, 12, 16, 20$  against the order  $L$ .

theory works well for our test-model  $Z(g)$ .

A better selection of the optimal  $\Omega$  values comes from the following observation. The imaginary parts of the approximations near the singularity at  $g = 0$  show tiny oscillations. The exact imaginary part is known to decrease extremely fast, like  $\exp(1/4g)$ , for  $g \rightarrow 0^-$ , practically without oscillations. We can make the tiny oscillations more visible by taking this exponential factor out of the imaginary part. This is done in Fig. 19. The oscillations differ strongly for different choices of  $\Omega^{(L)}$  from the central region of the cluster. To each order  $L$  we see that one of them is smoothest in the sense that the approximation approaches the singularity most closely before oscillations begin. If this  $\Omega^{(L)}$  is chosen as the optimal one, we obtain excellent results for the entire non-Borel-summable region  $g < 0$ . As an example, we pick the best zero for the  $L = 16$ th order. Fig. 19 shows the normalized imaginary part calculated

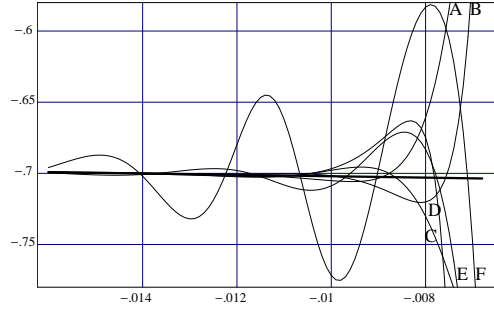


Figure 19: Normalized imaginary part  $\text{Im}[Z_{\text{var}}^{(16)}(g) \exp(-1/4g)]$  as a function of  $g$  based on six different complex zeros (thin curves). The fat curve represents the exact value, which is  $Z_{\text{exact}}(g) \simeq -0.7071 + .524g - 1.78g^2$ . Oscillations of varying strength can be observed near  $g = 0$ . Curves A and C carry most smoothly near up to the origin. Evaluation based on either of them yields equally good results. We have selected the zero belonging to curve C as our best choice to this order  $L = 16$ .

to this order, but based on different zeros from the central cluster. Curve C appears optimal. Therefore we select the underlying zero as our best choice at order  $L = 16$  and calculate with it real and imaginary part for the non-Borel-summable region  $-2 < g < -.008$ , to be compared with the exact values. Both are shown in Fig. 20, where we have again renormalized the imaginary part by the exponential factor  $\exp(-1/4g)$ . The agreement with the exact result (solid curve) is excellent as was to be expected because of the fast convergence observed in Fig. 16. It is indeed much better than the strong-coupling expansion to the same order, shown as a dashed curve. This is the essential improvement of our present theory as compared to previously known methods probing into the tunneling regime [51].

This non-Borel-summable regime will now be investigated for the quantum-mechanical anharmonic oscillator.

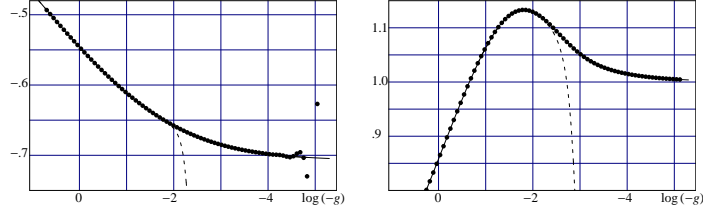


Figure 20: Normalized imaginary part  $\text{Im}[Z_{\text{var}}^{(16)}(g) \exp(-1/4g)]$  to the left and the real part  $\text{Re}[Z_{\text{var}}^{(16)}(g)]$  to the right, based on the best zero  $C$  from Fig. 19, are plotted against  $\log|g|$  as dots. The solid curve represents the exact function. The dashed curve is the 16th order of the strong-coupling expansion  $Z_{\text{strong}}^{(L)}(g)$  of equation (74).

## 6.2. Tunneling Regime of Quantum-Mechanical Anharmonic Oscillator

The divergent weak-coupling perturbation expansion for the ground state energy of the anharmonic oscillator in the potential  $V(x) = x^2/2 + g x^4$  to order  $L$

$$E_{0,\text{weak}}^{(L)}(g) = \sum_{l=0}^L a_l g^l, \quad (97)$$

where  $a_l = (1/2, 3/4, -21/8, 333/16, -30885/128, \dots)$ , is non-Borel-summable for  $g < 0$ . It may be treated in the same way as  $Z(g)$  of the previous model, making use as before of Eqs. (91)–(94), provided we set  $p = 1$  and  $\omega = 2/3$ , so that  $q = 3$ , accounting for the correct power behavior  $E_0(g) \propto g^{1/3}$  for  $g \rightarrow \infty$ . According to the principle of minimal dependence and oscillations, we pick a best zero for the order  $L = 64$  from the cluster of zeros of  $P_L(\sigma)$ , and use it to calculate the logarithm of the normalized imaginary part:

$$f(g) := \log \left[ \sqrt{-\pi g/2} E_{0,\text{var}}^{(64)}(g) \right] - 1/3g. \quad (98)$$

This quantity is plotted in Fig. 21 against  $\log(-g)$  close to the tip of the left-hand cut for  $-0.2 < g < -0.006$ . Comparing

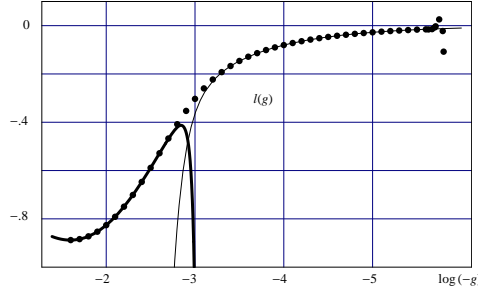


Figure 21: Logarithm of the imaginary part of the ground state energy of the anharmonic oscillator with the essential singularity factored out for better visualization,  $l(g) = \log \left[ \sqrt{-\pi g/2} E_{0,\text{var}}^{(64)}(g) \right] - 1/3g$ , plotted against small negative values of the coupling constant  $-0.2 < g < -0.006$  where the series is non-Borel-summable. The thin curve represents the divergent expansion around a critical bubble of Ref. [52]. The fat curve is the 22nd order approximation of the strong-coupling expansion, analytically continued to negative  $g$  in the sliding regime calculated in Chapter 17 of the textbook [6].

our result to older values from semi-classical calculations [52]

$$f(g) = b_1 g - b_2 g^2 + b_3 g^3 - b_4 g^4 + \dots, \quad (99)$$

with

$$b_1 = 3.95833 \quad b_2 = 19.344 \quad b_3 = 174.21 \quad b_4 = 2177, \quad (100)$$

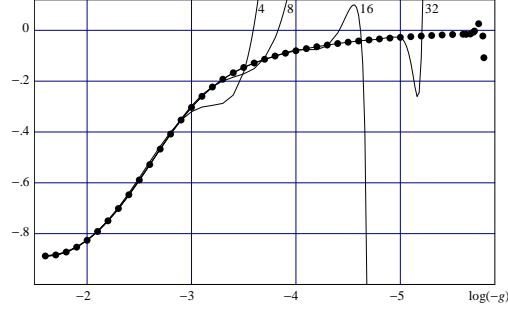


Figure 22: Logarithm of the normalized imaginary part of the ground state energy  $\log(\sqrt{-\pi g/2} E_{0,\text{var}}^L(g)) - 1/3g$ , plotted against  $\log(-g)$  for orders  $L = 4, 8, 16, 32$  (curves). It is compared with the corresponding results for  $L = 64$  (points). This is shown for small negative values of the coupling constant  $-0.2 < g < -0.006$ , i.e. in the non-Borel-summable critical-bubble region. Fast convergence is easily recognized. Lower orders oscillate more heavily. Increasing orders allow closer approach to the singularity at  $g = 0-$ .

shown in Fig. 21 as a thin curve, we find very good agreement. This expansion contains the information on the fluctuations around the critical bubble. It is divergent and non-Borel-summable for  $g < 0$ . In Appendix B we have rederived it in a novel way which allowed us to extend and improve it considerably.

Remarkably, our theory allows us to retrieve the first three terms of this expansion from the perturbation expansion. Since our result provides us with a regular approximation to the essential singularity, the fitting procedure depends somewhat on the interval over which we fit our curve by a power series. A compromise between a sufficiently long interval and the runaway of the divergent critical-bubble expansion is obtained for a lower limit  $g > -.0229 \pm .0003$  and an upper limit  $g = -0.006$ . Fitting a polynomial to the data, we extract the following first three coefficients:

$$b_1 = 3.9586 \pm .0003 \quad b_2 = 19.4 \pm .12 \quad b_3 = 135 \pm 18. \quad (101)$$

The agreement of these numbers with those in (99) demonstrates that our method is capable of probing deeply into the critical-bubble region of the coupling constant.

Further evidence for the quality of our theory comes from a comparison with the analytically continued strong-coupling result plotted to order  $L = 22$  as a fat curve in Fig. 21. This expansion was derived by a procedure of summing non-Borel-summable series developed in Chapter 17 of the textbook [6]. It was based on a two-step process: the derivation of a strong-coupling expansion of the type (74) from the divergent weak-coupling expansion, and an analytic continuation of the strong-coupling expansion to negative  $g$ . This method was applicable only for large enough coupling strength where the strong-coupling expansion converges, the so-called *sliding regime*. It could not invade into the tunneling regime at small  $g$  governed by critical bubbles, which was treated in [6] by a separate variational procedure. The present work fills the missing gap by extending variational perturbation theory to *all*  $g$  arbitrarily close to zero, without the need for a separate treatment of the tunneling regime.

It is interesting to see, how the correct limit is approached as the order  $L$  increases. This is shown in Fig. 22, based on the optimal zero in each order. For large negative  $g$ , even the small orders give excellent results. Close to the singularity the scaling factor  $\exp(-1/3g)$  will always win over the perturbation results. It is surprising, however, how fantastically close to the singularity we can go.

### 6.3. Dynamic Approach to the Critical-Bubble Regime

Regarding the computational challenges connected with the critical-bubble regime of small  $g < 0$ , it is worth to develop an independent method to calculate imaginary parts in the tunneling regime. For a quantum-mechanical system with an interaction potential  $g V(x)$ , such as a the harmonic oscillator, we may study the effect of an infinitesimal increase in  $g$  upon the system. It induces an infinitesimal unitary transformation of the Hilbert space. The new Hilbert space can be made the starting point for the next infinitesimal increase in  $g$ . In this way we derive an infinite set of first order ordinary differential equations for the change of the energy levels and matrix elements (for details see Appendix C):

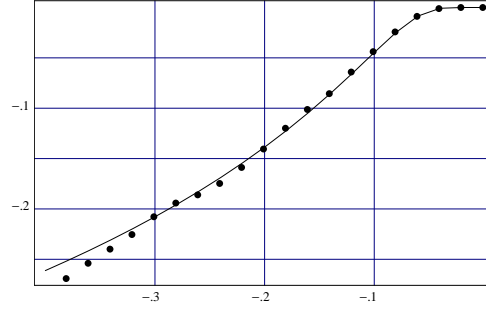


Figure 23: inary part of the ground state energy of the anharmonic oscillator as solution of the coupled set of differential equations (102), truncated at the energy level of  $n = 64$  (points), compared with the corresponding quantity from the  $L = 64$ th order of non-Borel-summable variational perturbation theory (curve), both shown as functions of the coupling constant  $g$ .

$$E'_n(g) = V_{nn}(g), \quad (102)$$

$$V'_{mn}(g) = \sum_{k \neq n} \frac{V_{mk}(g)V_{kn}(g)}{E_m(g) - E_k(g)} + \sum_{k \neq m} \frac{V_{mk}(g)V_{kn}(g)}{E_n(g) - E_k(g)}. \quad (103)$$

This system of equations holds for any one-dimensional Schroedinger problem. Individual differences come from the initial conditions, which are the energy levels  $E_n(0)$  of the unperturbed system and the matrix elements  $V_{nm}(0)$  of the interaction  $V(x)$  in the unperturbed basis. For a numerical integration of the system a truncation is necessary. The obvious way is to restrict the Hilbert space to the manifold spanned by the lowest  $N$  eigenvectors of the unperturbed system. For cases like the anharmonic oscillator, which are even, with even perturbation and with only an even state to be investigated, we may span the Hilbert space by even basis vectors only. Our initial conditions are thus for  $n = 0, 1, 2, \dots, N/2$ :

$$E_{2n}(0) = 2n + 1/2 \quad (104)$$

$$V_{2n,2m} = 0 \quad \text{if } m < 0 \text{ or } m > N/2 \quad (105)$$

$$V_{2n,2n}(0) = 3(8n^2 + 4n + 1)/4 \quad (106)$$

$$V_{2n,2n \pm 2}(0) = (4n + 3) \sqrt{(2n + 1)(2n + 2)}/2 \quad (107)$$

$$V_{2n,2n \pm 4}(0) = \sqrt{(2n + 1)(2n + 2)(2n + 3)(2n + 4)}/4 \quad (108)$$

$$(109)$$

For the anharmonic oscillator with a  $V(x) = x^4$  potential, all sums in equation (102) are finite with at most four terms due to the near-diagonal structure of the perturbation.

In order to find a solution for some  $g < 0$ , we first integrate the system from 0 to  $|g|$ , then around a semi-circle  $g = |g| \exp(i\varphi)$  from  $\varphi = 0$  to  $\varphi = \pi$ . The imaginary part of  $E_0(g)$  obtained from a calculation with  $N = 64$  is shown in Fig. 23, where it is compared with the variational result for  $L = 64$ . The agreement is excellent. It must be noted, however, that the necessary truncation of the system of differential equations introduces an error, which cannot be made arbitrarily small by increasing the truncation limit  $N$ . The approximations are asymptotic sharing this property with the original weak-coupling series. Its divergence is, however, reduced considerably, which is the reason why we obtain accurate results for the critical-bubble regime, where the weak-coupling series fails completely to reproduce the imaginary part.

## 7. Hydrogen Atom in Strong Magnetic Field

A point particle in  $D$  dimensions with a potential  $V(\mathbf{x})$  and a vector potential  $\mathbf{A}(\mathbf{x})$  is described by a Hamiltonian

$$H(\mathbf{p}, \mathbf{x}) = \frac{1}{2M} \left[ \mathbf{p} - \frac{e}{c} \mathbf{A}(\mathbf{x}) \right]^2 - \frac{e^2}{4\pi|\mathbf{x}|}. \quad (110)$$

The quantum statistical partition function is given by the euclidean phase space path integral

$$Z = \oint \mathcal{D}'^D x \mathcal{D}^D p e^{-\mathcal{A}[\mathbf{p}, \mathbf{x}]/\hbar} \quad (111)$$

with an action

$$\mathcal{A}[\mathbf{p}, \mathbf{x}] = \int_0^{\hbar\beta} d\tau [-i\mathbf{p}(\tau) \cdot \dot{\mathbf{x}}(\tau) + H(\mathbf{p}(\tau), \mathbf{x}(\tau))], \quad (112)$$

and the path measure

$$\oint \mathcal{D}'^D x \mathcal{D}^D p = \lim_{N \rightarrow \infty} \prod_{n=1}^{N+1} \left[ \int \frac{d^D x_n d^D p_n}{(2\pi\hbar)^D} \right]. \quad (113)$$

The parameter  $\beta = 1/k_B T$  denotes the usual inverse thermal energy at temperature  $T$ , where  $k_B$  is the Boltzmann constant. From  $Z$  we obtain the free energy of the system:

$$F = -\frac{1}{\beta} \ln Z. \quad (114)$$

Applying variational perturbation theory to the path integral (111) leads to a variational binding energy [54] defined by  $\varepsilon(B) \equiv B/2 - E(B)$  in atomic natural with  $\hbar = 1$ ,  $M = 1$ ,  $e = 1$ , energies in units of 2 Ryd =  $e^4 M^2 / \hbar^3$ .

$$\varepsilon_{\eta, \Omega}^{(1)}(B) = \frac{B}{2} - \frac{\Omega}{4} \left( 1 + \frac{\eta}{2} \right) - \frac{B^2}{4\Omega} - \sqrt{\frac{\eta\Omega}{2\pi}} h(\eta) \quad (115)$$

with

$$h(\eta) = \frac{1}{\sqrt{1-\eta}} \ln \frac{1 - \sqrt{1-\eta}}{1 + \sqrt{1-\eta}}. \quad (116)$$

Here we have introduced variational parameters

$$\eta \equiv \frac{2\Omega_{\parallel}}{\Omega_{\perp 2}} \leq 1, \quad \Omega \equiv \Omega_{\perp 2}. \quad (117)$$

Extremizing the energy with respect to these yields the conditions

$$\begin{aligned} \frac{\Omega}{8} + \sqrt{\frac{\Omega}{2\pi\eta}} \frac{1}{1-\eta} \left( 1 + \frac{1}{2} \frac{1}{\sqrt{1-\eta}} \ln \frac{1 - \sqrt{1-\eta}}{1 + \sqrt{1-\eta}} \right) &\stackrel{!}{=} 0, \\ \frac{1}{4} + \frac{\eta}{8} - \frac{B^2}{4\Omega^2} + \frac{1}{2} \sqrt{\frac{\eta}{2\pi\Omega}} \frac{1}{\sqrt{1-\eta}} \ln \frac{1 - \sqrt{1-\eta}}{1 + \sqrt{1-\eta}} &\stackrel{!}{=} 0. \end{aligned} \quad (118)$$

Expanding the variational parameters into perturbation series of the square magnetic field  $B^2$ ,

$$\eta(B) = \sum_{n=0}^{\infty} \eta_n B^{2n}, \quad \Omega(B) = \sum_{n=0}^{\infty} \Omega_n B^{2n} \quad (119)$$

and inserting these expansions into the self-consistency conditions (118) and (118) we obtain order by order the coefficients given in Table 2. Inserting these values into the expression for the binding energy (115) and expand with respect to  $B^2$ , we obtain the perturbation series

$$\varepsilon^{(1)}(B) = \frac{B}{2} - \sum_{n=0}^{\infty} \varepsilon_n B^{2n}. \quad (120)$$

The first coefficients are also given in Table 2. We find thus the important result that the first-order variational perturbation solution possesses a perturbative behavior with respect to the square magnetic field strength  $B^2$  in the

Table 2: Perturbation coefficients up to order  $B^6$  for the weak-field expansions of the variational parameters and the binding energy in comparison to the exact ones of Ref. [55].

$n$	0	1	2	3
$\eta_n$	1.0	$-\frac{405\pi^2}{7168} \approx -0.5576$	$\frac{16828965\pi^4}{1258815488} \approx 1.3023$	$-\frac{3886999332075\pi^6}{884272562962432} \approx -4.2260$
$\Omega_n$	$\frac{32}{9\pi} \approx 1.1318$	$\frac{99\pi}{224} \approx 1.3885$	$-\frac{1293975\pi^3}{19668992} \approx -2.03982$	$\frac{524431667187\pi^5}{27633517592576} \approx 5.8077$
$\varepsilon_n$	$-\frac{4}{3\pi} \approx -0.4244$	$\frac{9\pi}{128} \approx 0.2209$	$-\frac{8019\pi^3}{1835008} \approx -0.1355$	$\frac{256449807\pi^5}{322256764928} \approx 0.2435$
$\varepsilon_n$ [55]	-0.5	0.25	$-\frac{53}{192} \approx -0.2760$	$\frac{5581}{4608} \approx 1.2112$

weak-field limit thus yielding the correct asymptotic. The coefficients differ in higher order from the exact ones but are improved by variational perturbation theory [6].

In a strong magnetic field one has

$$\Omega_{\perp} \gg 2\Omega_{\parallel}, \quad \Omega_{\parallel} \ll B \quad (121)$$

and the variational expression simplifies to

$$\varepsilon_{\Omega_{\perp}, \Omega_{\parallel}}^{(1)} = \frac{B}{2} - \left( \frac{\Omega_{\perp}}{4} + \frac{B^2}{4\Omega_{\perp}} + \frac{\Omega_{\parallel}}{4} + \sqrt{\frac{\Omega_{\parallel}}{\pi}} \ln \frac{\Omega_{\parallel}}{2\Omega_{\perp}} \right), \quad (122)$$

which is minimal at

$$\sqrt{\Omega_{\parallel}} = -\frac{2}{\sqrt{\pi}} (\ln \Omega_{\parallel} - \ln \Omega_{\perp} + 2 - \ln 2), \quad (123)$$

$$\Omega_{\perp} = 2\sqrt{\frac{\Omega_{\parallel}}{\pi}} + B\sqrt{1 + 4\frac{\Omega_{\parallel}}{\pi B^2}}. \quad (124)$$

Expanding the second conditions as

$$\Omega_{\perp} = B + 2\sqrt{\frac{\Omega_{\parallel}}{\pi}} + 2\frac{\Omega_{\parallel}}{\pi B} - 4\frac{\Omega_{\parallel}^2}{\pi^2 B^3} + \dots, \quad (125)$$

and inserting only the first two terms into the first condition (123), we neglect terms of order  $1/B$ , and find

$$\sqrt{\Omega_{\parallel}} \approx \frac{2}{\sqrt{\pi}} (\ln B - \ln \Omega_{\parallel}^{(1)} + \ln 2 - 2). \quad (126)$$

To obtain a tractable approximation for  $\Omega_{\parallel}$ , we perform some iterations starting from

$$\sqrt{\Omega_{\parallel}^{(1)}} = \frac{2}{\sqrt{\pi}} \ln 2Be^{-2} \quad (127)$$

Reinserting this on the right-hand side of Eq. (126), one obtains the second iteration  $\sqrt{\Omega_{\parallel}^{(2)}}$ . We stop this procedure after an additional reinsertion which yields

$$\sqrt{\Omega_{\parallel}^{(3)}} = \frac{2}{\sqrt{\pi}} \left( \ln 2Be^{-2} - 2\ln \left[ \frac{2}{\sqrt{\pi}} \left\{ \ln 2Be^{-2} - 2\ln \left( \frac{2}{\sqrt{\pi}} \ln 2Be^{-2} \right) \right\} \right] \right). \quad (128)$$

The reader may convince himself that this iteration procedure indeed converges. For a subsequent systematical extraction of terms essentially contributing to the binding energy, the expression (128) is not satisfactory. Therefore it is better to separate the leading term in the curly brackets and expand the logarithm of the remainder. Then this procedure is applied to the expression in the square brackets and so on. Neglecting terms of order  $\ln^{-3} B$ , we obtain

$$\sqrt{\Omega_{\parallel}^{(3)}} \approx \frac{2}{\sqrt{\pi}} \left( \ln 2Be^{-2} + \ln \frac{\pi}{4} - 2\ln \ln 2Be^{-2} \right). \quad (129)$$

Table 3: Example for the competing leading six terms in Eq. (134) at  $B = 10^5 B_0 \approx 2.35 \times 10^{14}$  G.

$(1/\pi)\ln^2 B$	$-(4/\pi)\ln B \ln \ln B$	$(4/\pi)\ln^2 \ln B$	$-(4b/\pi)\ln \ln B$	$[2(b+2)/\pi]\ln B$	$b^2/\pi$
42.1912	-35.8181	7.6019	4.8173	3.3098	0.7632

The double-logarithmic term can be expanded in a similar way as described above:

$$\ln \ln 2Be^{-2} = \ln \left[ \ln B \left( 1 + \frac{\ln 2 - 2}{\ln B} \right) \right] = \ln \ln B + \frac{\ln 2 - 2}{\ln B} - \frac{1}{2} \frac{(\ln 2 - 2)^2}{\ln^2 B} + O(\ln^{-3} B). \quad (130)$$

Thus the expression (129) may be rewritten as

$$\sqrt{\Omega_{\parallel}^{(3)}} = \frac{2}{\sqrt{\pi}} \left( \ln B - 2 \ln \ln B + \frac{2a}{\ln B} + \frac{a^2}{\ln^2 B} + b \right) + O(\ln^{-3} B) \quad (131)$$

with abbreviations

$$a = 2 - \ln 2 \approx 1.307, \quad b = \ln \frac{\pi}{2} - 2 \approx -1.548. \quad (132)$$

The first observation is that the variational parameter  $\Omega_{\parallel}$  is always much smaller than  $\Omega_{\perp}$  in the high  $B$ -field limit. Thus we can further simplify the approximation (125) by replacing

$$\Omega_{\perp} \approx B \left( 1 + \frac{2}{B} \sqrt{\frac{\Omega_{\parallel}}{\pi}} \right) \rightarrow B \quad (133)$$

without affecting the following expression for the binding energy. Inserting the solutions (131) and (133) into the equation for the binding energy (122) and expanding the logarithmic term once more as described, we find up to the order  $\ln^{-2} B$ :

$$\begin{aligned} \varepsilon^{(1)}(B) &= \frac{1}{\pi} \left( \ln^2 B - 4 \ln B \ln \ln B + 4 \ln^2 \ln B - 4b \ln \ln B + 2(b+2) \ln B + b^2 - \frac{1}{\ln B} [8 \ln^2 \ln B - 8b \ln \ln B + 2b^2] \right) \\ &\quad + O(\ln^{-2} B) \end{aligned} \quad (134)$$

Note that the prefactor  $1/\pi$  of the leading  $\ln^2 B$ -term differs from a value  $1/2$  obtained by Landau and Lifschitz [56]. Our different value is a consequence of using a harmonic trial system. The calculation of higher orders in variational perturbation theory would improve the value of the prefactor.

At a magnetic field strength  $B = 10^5 B_0$ , which corresponds to  $2.35 \times 10^{10} \text{ T} = 2.35 \times 10^{14} \text{ G}$ , the contribution from the first six terms is 22.87 [2 Ryd]. The next three terms suppressed by a factor  $\ln^{-1} B$  contribute  $-2.29$  [2 Ryd], while an estimate for the  $\ln^{-2} B$ -terms yields nearly  $-0.3$  [2 Ryd]. Thus we find

$$\varepsilon^{(1)}(10^5) = 20.58 \pm 0.3 \text{ [2 Ryd]}. \quad (135)$$

This is in very good agreement with the value 20.60 [2 Ryd] obtained from an accurate numerical treatment [58].

Table 3 lists the values of the first six terms of Eq. (134). This shows in particular the significance of the second-leading term  $-(4/\pi)\ln B \ln \ln B$ , which is of the same order of the leading term  $(1/\pi)\ln^2 B$  but with an opposite sign. In Fig. 24, we have plotted the expression

$$\varepsilon_L(B) = \frac{1}{2} \ln^2 B \quad (136)$$

from Landau and Lifschitz [56] to illustrate that it gives far too large binding energies even at very large magnetic fields, e.g. at  $2000 B_0 \propto 10^{12} \text{ G}$ .

This strength of magnetic field appears on surfaces of neutron stars ( $10^{10} - 10^{12} \text{ G}$ ). A recently discovered new type of neutron star is the so-called magnetar. In these, charged particles such as protons and electrons produced by decaying neutrons give rise to the giant magnetic field of  $10^{15} \text{ G}$ . Magnetic fields of white dwarfs reach only up to  $10^6 - 10^8 \text{ G}$ . All these magnetic field strengths are far from realization in experiments. The strongest magnetic fields



ever produced in a laboratory were only of the order  $10^5$  G, an order of magnitude larger than the fields in sun spots which reach about  $0.4 \times 10^4$  G. Recall, for comparison, that the earth's magnetic field has the small value of 0.6 G.

The nonleading terms in Eq. (134) give important contributions to the asymptotic behavior even at such large magnetic fields, as we can see in Fig. 24. It is an unusual property of the asymptotic behavior that the absolute value of the difference between the Landau-expression (136) and our approximation (134) diverges with increasing magnetic field strengths  $B$ , only the relative difference decreases.

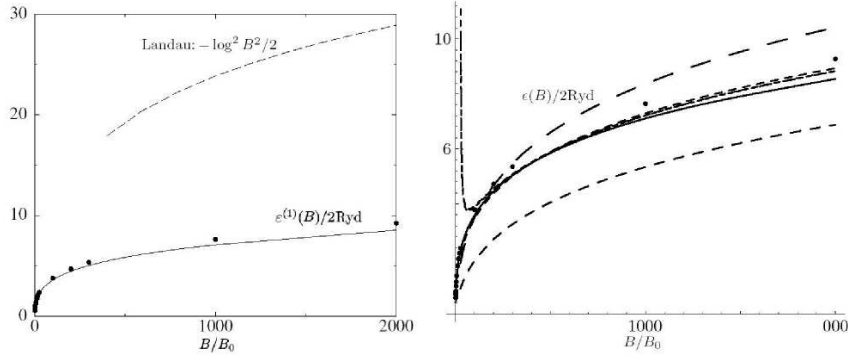


Figure 24: Ground state energy  $E(B)$  of hydrogen in a strong magnetic field. The dotted figure on the left is Landau's old upper limit. On the right-hand side our curve is compared with the accurate values (dots [57, 58]). It also shows various lower-order approximations within our procedure. The quantity  $\varepsilon(B)$  is the binding energy defined by  $\varepsilon(B) \equiv B/2 - E(B)$ . All quantities are in atomic natural units  $\hbar = 1$ ,  $M = 1$ ,  $e = 1$ , energies in units of  $2 \text{ Ryd} = e^4 M^2 / \hbar^3$ .

## 8. Appendix A: Modification of Principle of Minimal Sensitivity

The naive quantum mechanical variational perturbation theory has been used by many authors under the name  $\delta$ -expansion. This name stems from the fact that one may write the Hamiltonian of an anharmonic oscillator

$$H = \frac{p^2}{2M} + \frac{M}{2} \omega^2 x^2 + \frac{g}{4} x^4 \quad (137)$$

alternatively as

$$H = \frac{p^2}{2M} + M \frac{\Omega^2}{2} x^2 + \delta \left[ \frac{M}{2} (\omega^2 - \Omega^2) + \frac{g}{4} x^4 \right], \quad (138)$$

and expand the eigenvalues systematically in powers of  $\delta$ . Each partial sum of order  $L$  is evaluated at  $\delta = 1$  and extremized in  $\Omega$ . It is obvious that this procedure is equivalent to the re-expansion method in Section 2.

As mentioned in the text and pointed out in [16], such an analysis is inapplicable in quantum field theory, where the Wegner exponent  $\omega$  is anomalous and must be determined dynamically. Most recently, the false treatment was given to the shift of the critical temperature in a Bose-Einstein condensate caused by a small interaction [50, 29, 41]. We have seen in Section 4 that the perturbation expansion for this quantity is a function of  $g/\mu$  where  $\mu$  is the chemical potential which goes to zero at the critical point, we are faced with a typical strong-coupling problem of critical phenomena. In order to justify the application of the  $\delta$ -expansion to this problem, BR [50] studied the convergence properties of the method by applying it to a certain amplitude  $\Delta(g)$  of an  $O(N)$ -symmetric  $\phi^4$ -field theory in the limit of large  $N$ , where the model is exactly solvable.

Their procedure must be criticized in two ways. First, the amplitude  $\Delta(g)$  they considered is not a good candidate for a resummation by a  $\delta$ -expansion since it does not possess the characteristic strong-coupling power structure [15] of quantum mechanics and field theory, which the final resummed expression will always have by construction. The power structure is disturbed by additional logarithmic terms. Second, the  $\delta$ -expansion is, in the example, equivalent to choosing, on dimensional grounds, the exponent  $\omega = 2$  in [15], which is far from the correct value  $\approx 0.843$  to be derived below. Thus the  $\delta$ -expansion is inapplicable, and this explains the problems into which BR run in their

resummation attempt. Most importantly, they do not find a well-shaped plateau of the variational expressions  $\Delta^{(L)}(g, z)$  as a function of  $z$  which would be necessary for invoking the principle of minimal sensitivity. Instead, they observe that the zeros of the first derivatives  $\partial_z \Delta^{(L)}(g, z)$  run away far into the complex plain. Choosing the complex solutions to determine their final resummed value misses the correct one by 3% up to the 35th order.

One may improve the situation by trying out various different  $\omega$ -values and choosing the best of them yielding an acceptable plateau in  $\Delta(g, z)$ . This happens for  $\omega \approx 0.843$ . However, even for this optimal value, the resummation result never converges to the correct limit. For  $\Delta(g)$  the error happens to be numerically small, only 0.1%, but it will be uncontrolled in physical problems where the result is unknown.

Let us explain these points in more detail. BR consider the weak-coupling series with the reexpansion parameter  $\delta$ :

$$\Delta(\delta, g) = - \sum_{l=1}^{\infty} \left( - \frac{\delta g}{\sqrt{1-\delta}} \right)^l a_l, \quad \text{where } a_l \equiv \int_0^{\infty} K(x) f^l(x) dx, \quad (139)$$

with

$$K(x) \equiv \frac{4x^2}{\pi(1+x^2)^2}, \quad f(x) \equiv \frac{2}{x} \arctan \frac{x}{2}. \quad (140)$$

The geometric series in (139) can be summed exactly, and the result may formally be reexpanded into a strong-coupling series in  $h \equiv \sqrt{1-\delta}/(\delta g)$ :

$$\Delta(\delta, g) = \int_0^{\infty} K(x) \frac{\delta g f(x)}{\sqrt{1-\delta} + \delta g f(x)} dx = \sum_{m=0}^{\infty} b_m (-h)^m, \quad \text{where } b_m = \int_0^{\infty} K(x) f^{-m}(x) dx. \quad (141)$$

The strong-coupling limit is found for  $h \rightarrow 0$  where  $\Delta \rightarrow b_0 = \int_0^{\infty} dx K(x) = 1$ . The approach to this limit is, however, *not* given by a strong-coupling expansion of the form (141). This would only happen if all the integrals  $b_m$  were to exist which, unfortunately, is not the case since all integrals for  $b_m$  with  $m > 0$  diverge at the upper limit, where

$$f(x) = \frac{2}{x} \arctan \frac{x}{2} \sim \frac{\pi}{x}. \quad (142)$$

The exact behavior of  $\Delta$  in the strong-coupling limit  $h \rightarrow 0$  is found by studying the effect of the asymptotic  $\pi/x$ -contribution of  $f(x)$  to the integral in (141). For  $f(x) = \pi/x$  we obtain

$$\int_0^{\infty} K(x) \frac{1}{1 + h/f(x)} dx = \frac{\pi^4 + 2\pi h - \pi h + 2h + 4\pi h \log h/\pi}{(\pi + h)}. \quad (143)$$

The logarithm of  $h$  shows a mismatch with the general asymptotic form of the result [15], which and prevents the expansion (139) to be a candidate for variational perturbation theory.

We now explain the second criticism. Suppose we ignore the just-demonstrated fundamental obstacle and follow the rules of the  $\delta$ -expansion, defining the  $L$ th order approximant  $\Delta(\delta, \infty)$  by expanding (139) in powers of  $\delta$  up to order  $\delta^L$ , setting  $\delta = 1$ , and defining  $z \equiv g$ . Then we obtain the  $L$ th variational expression for  $b_0$ :

$$b_0^{(L)}(\omega, z) = \sum_{l=1}^L a_l z^l \binom{L-l+l/\omega}{L-l}, \quad (144)$$

with  $\omega = 2$ , to be optimized in  $z$ . This  $\omega$ -value would only be adequate if the approach to the strong-coupling limit behaved like  $A + B/h^2 + \dots$ , rather than (143). This is the reason why BR find no real regime of minimal sensitivity on  $z$ .

Let us attempt to improve the situation by determining  $\omega$  dynamically by making the plateau in the plots of  $\Delta^{(L)}(\omega, h)$  versus  $h$  horizontal for several different  $\omega$ -values. The result is  $\omega \approx 0.843$ , quite far from the naive value 2. This value can also be estimated by inspecting plots of  $\Delta^{(L)}(\omega, h)$  versus  $h$  for several different  $\omega$ -values in Fig. 25, and selecting the one producing minimal sensitivity. It produces reasonable results also in higher orders, as is seen in

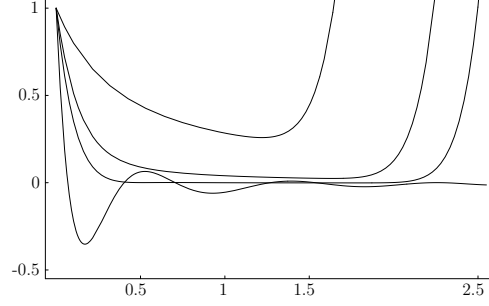


Figure 25: Plot of  $1 - b_0^{(L)}(\omega, z)$  versus  $z$  for  $L = 10$  and  $\omega = 0.6, 0.843, 1, 2$ . The curve with  $\omega = 0.6$  shows oscillations. They decrease with increasing  $\omega$  and becomes flat at about  $\omega = 0.843$ . Further increase of  $\omega$  tilts the plateau and shows no regime of minimal sensitivity. At the same time, the minimum of the curve rises rapidly above the correct value of  $1 - b_0 = 0$ , as can be seen from the upper two curves for  $\omega = 1$  and  $\omega = 2$ , respectively.

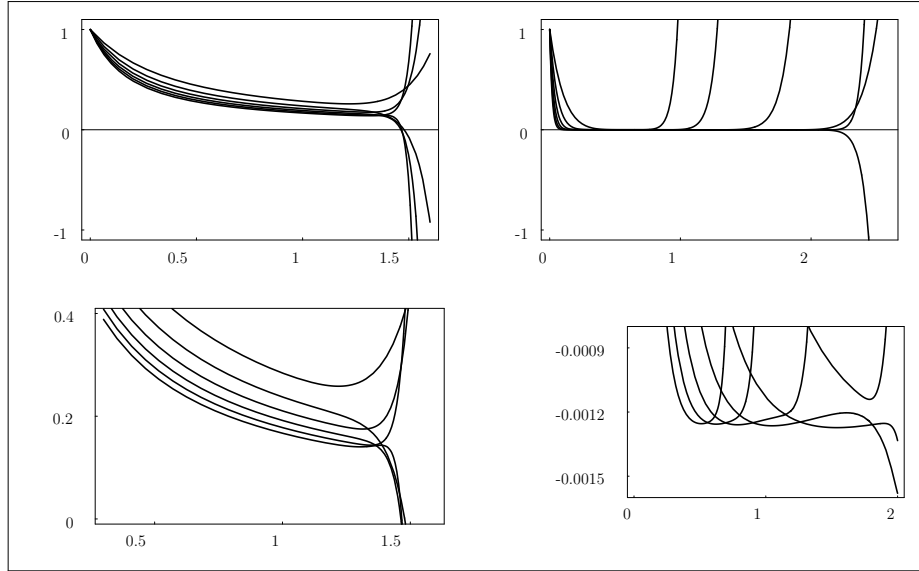


Figure 26: Left-hand column shows plots of  $1 - b_0^{(L)}(\omega, z)$  for  $L = 10, 17, 24, 31, 38, 45$  with  $\omega = 2$  of  $\delta$ -expansion of BR, right-hand column with optimal  $\omega = 0.843$ . The lower row enlarges the interesting plateau regions of the plots above. Only the right-hand side shows minimal sensitivity, and the associated plateau lies closer to the correct value  $1 - b_0 = 0$  than the minima in the left column by two orders of magnitude. Still the right-hand curves do not approach the exact limit for  $L \rightarrow \infty$  due to the wrong strong-coupling behavior of the initial function.

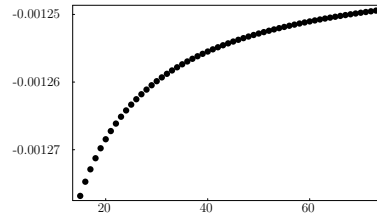


Figure 27: Deviation of  $1 - b_{0,\text{plateau}}^{(L)}(\omega = 0.843)$  from zero as a function of the order  $L$ . Asymptotically the value  $-0.00136$  is reached, missing the correct number by about 0.1%.

Fig. 26. The approximations appear to converge rapidly. But the limit does not coincide with the known exact value, although it happens to lie numerically quite close. Extrapolating the successive approximations by an extremely accurate fit to the analytically known large-order behavior [15] with a function  $b_{0,\text{plateau}}^{(L)}(\omega = 0.843) = A + B L^{-\kappa}$ , we find convergence to  $A = 1 - 0.001136$ , which misses the correct limit  $A = 1$ . The other two parameters are fitted best by  $B = -0.002495$  and  $\kappa = 0.922347$  (see Fig. 27).

We may easily convince ourselves by numerical analysis that the error in the limiting value is indeed linked to the failure of the strong-coupling behavior (143) to have the power structure of [15]. For this purpose we change the function  $f(x)$  in equation (140) slightly into  $\tilde{f}(x) = f(x) + 1$ , which makes the integrals for  $\tilde{b}_m$  in (141) convergent. The exact limiting value 1 of  $\tilde{A}$  remains unchanged, but  $\tilde{b}_0^{(L)}$  acquires now the correct strong-coupling power structure of [15]. For this reason, we can easily verify that the application of variational theory with a dynamical determination of  $\omega$  yields the correct strong-coupling limit 1 with the exponentially fast convergence of the successive approximations for  $L \rightarrow \infty$  like  $\tilde{b}_0^{(L)} \approx 1 - \exp(-1.909 - 1.168 L)$ .

It is worthwhile emphasizing that an escape to complex zeros which BR propose to remedy the problems of the  $\delta$ -expansion is really of no help. It has been claimed [53] and repeatedly cited [49], that the study of the anharmonic oscillator in quantum mechanics suggests the use of complex extrema to optimize the  $\delta$ -expansion. In particular, the use of so-called *families* of optimal candidates for the variational parameter  $z$  has been suggested. We are now going to show, that following these suggestions one obtains bad resummation results for the anharmonic oscillator. Thus we expect such procedures to lead to even worse results in field-theoretic applications.

In quantum mechanical applications there are no anomalous dimensions in the strong-coupling behavior of the energy eigenvalues. The growth parameters  $\alpha$  and  $\omega$  can be directly read off from the Schrödinger equation; they are  $\alpha = 1/3$  and  $\omega = 2/3$  for the anharmonic oscillator (see Appendix A). The variational perturbation theory is applicable for all couplings strengths  $g$  as long as  $b_0^{(L)}(z)$  becomes stationary for a certain value of  $z$ . For higher orders  $L$  it must exhibit a well-developed plateau. Within the range of the plateau, various derivatives of  $b_0^{(L)}(z)$  with respect to  $z$  will vanish. In addition there will be complex zeros with small imaginary parts clustering around the plateau. They are, however, of limited use for designing an automatized computer program for localizing the position of the plateau. The study of several examples shows that plotting  $b_0^{(L)}(z)$  for various values of  $\alpha$  and  $\omega$  and judging visually the plateau is by far the safest method, showing immediately which values of  $\alpha$  and  $\omega$  lead to a well-shaped plateau.

Let us review briefly the properties of the results obtained from real and complex zeros of  $\partial_z b_0^{(L)}(z)$  for the anharmonic oscillator. In Fig. 28, the logarithmic error of  $b_0^{(L)}$  is plotted versus the order  $L$ . At each order, all zeros of the first derivative are exploited. To test the rule suggested in [53], only the real parts of the complex roots have been used to evaluate  $b_0^{(L)}$ . The fat points represent the results of real zeros, the thin points stem from the real parts of complex zeros. It is readily seen that the real zeros give the better result. Only by chance may a complex zero yield a smaller error. Unfortunately, there is no rule to detect these accidental events. Most complex zeros produce large errors.

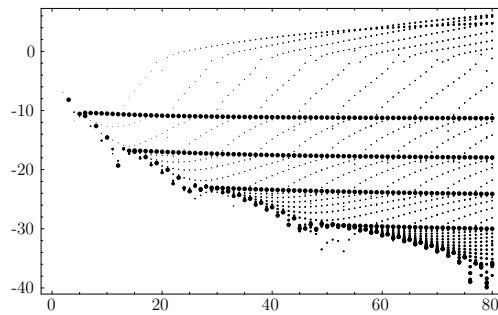


Figure 28: Logarithmic error of the leading strong-coupling coefficient  $b_0^{(L)}$  of the ground state energy of the anharmonic oscillator with  $x^4$  potential. The errors are plotted over the order  $L$  of the variational perturbation expansion. At each order, all zeros of the first derivative have been exploited. Only the real parts of the complex roots have been used to evaluate  $b_0^{(L)}$ . The fat points show results from real zeros, the smaller points those from complex zeros, size is decreasing with distance from real axis.

We observe the existence of families described in detail in the textbook [6] and rediscovered in Ref. [53]. These families start at about  $N = 6, 15, 30, 53$ , respectively. But each family fails to converge to the correct result. Only

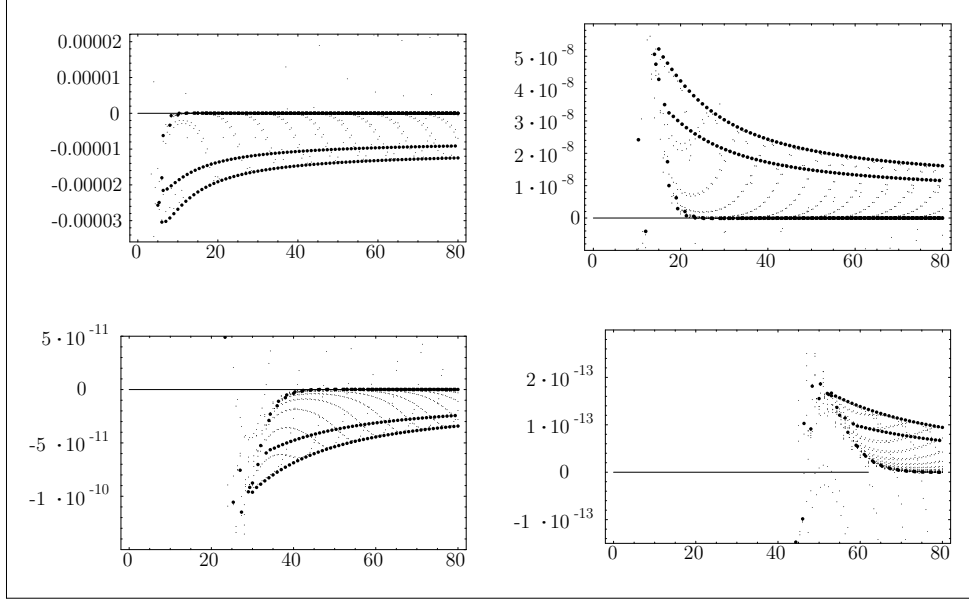


Figure 29: Deviation of the coefficient  $b_0^{(L)}$  from the exact value is shown as a function of perturbative order  $L$  on a linear scale. As before, fat dots represent real zeros. In addition to Fig. 28, the results obtained from zeros of the second derivative of  $b_0^{(L)}$  are shown. They give rise to own families with smaller errors by about 30%. At  $N = 6$ , the upper left plot shows the start of two families belonging to the first and second derivative of  $b_0^{(L)}$ , respectively. The deviations of both families are negative. On the upper right-hand figure, an enlargement visualizes the next two families starting at  $N = 15$ . Their deviations are positive. The bottom row shows two more enlargements of families starting at  $N = 30$  and  $N = 53$ , respectively. The deviations alternate again in sign.

a sequence of selected members in each family leads to an exponential convergence. Consecutive families alternate around the correct result, as can be seen more clearly in a plot of the deviations of  $b_0^{(L)}$  from their  $L \rightarrow \infty$ -limit in Fig. 29, where values derived from the zeros of the second derivative of  $b_0^{(L)}$  have been included. These give rise to accompanying families of similar behavior, deviating with the same sign pattern from the exact result, but lying closer to the correct result by about 30%.

## 9. Appendix B: Ground-State Energy from Imaginary Part

We determine the ground state energy function  $E_0(g)$  for the anharmonic oscillator on the cut, i.e. for  $g < 0$  in the bubble region, from the weak coupling coefficients  $a_l$  of equation (97). The behavior of the  $a_l$  for large  $l$  can be cast into the form

$$a_l/a_{l-1} = - \sum_{j=-1}^L \beta_j l^{-j}. \quad (145)$$

The  $\beta_j$  can be determined by a high precision fit to the data in the large  $l$  region of  $250 < l < 300$  to be

$$\beta_{-1, 0, 1, \dots} = \left\{ 3, -\frac{3}{2}, \frac{95}{24}, \frac{113}{6}, \frac{391691}{3456}, \frac{40783}{48}, \frac{1915121357}{248832}, \frac{10158832895}{124416}, \frac{70884236139235}{71663616}, \right. \\ \left. \frac{60128283463321}{4478976}, \frac{286443690892}{1423}, \frac{144343264152266}{43743}, \frac{351954117229}{6}, \frac{2627843837757582}{2339}, \right. \\ \left. \frac{230619387597863}{10}, \frac{12122186977970425}{24}, \frac{41831507430222441029}{3550}, \dots \right\}, \quad (146)$$

where the rational numbers up to  $j = 6$  are found to be exact, whereas the higher ones are approximations.

Equation (145) can be read as recurrence relation for the coefficients  $a_l$ . Now we construct an ordinary differential equation for  $E(g) := E_{0, \text{weak}}^{(L)}(g)$  from this recurrence relation and find:

$$\left[ \left( g \frac{d}{dg} \right)^L + g \sum_{j=0}^{L+1} \beta_{L-j} \left( g \frac{d}{dg} + 1 \right)^j \right] E(g) = 0. \quad (147)$$

All coefficients being real, real and imaginary part of  $E(g)$  each have to satisfy this equation separately. The point  $g = 0$ , however, is not a regular point. We are looking for a solution, which is finite when approaching it along the negative real axis. Asymptotically  $E(g)$  has to satisfy  $E(g) \simeq \exp(1/g\beta_{-1}) = \exp(1/3g)$ . Therefore we solve (147) with the ansatz

$$E(g) = g^\alpha \exp\left(\frac{1}{3g} - \sum_{k=1} b_k (-g)^k\right) \quad (148)$$

to obtain  $\alpha = -1/2$  and

$$b_{1,2,3,\dots} = \left\{ \frac{95}{24}, \frac{619}{32}, \frac{200689}{1152}, \frac{2229541}{1024}, \frac{104587909}{3072}, \frac{7776055955}{12288}, \frac{9339313153349}{688128}, \frac{172713593813181}{524288}, \right. \\ \left. \frac{1248602386820060039}{139886592}, \frac{14531808399402704160316631}{54391637278720}, \frac{12579836720279641736960567921}{1435939224158208}, \right. \\ \left. \frac{109051824717547897884794645746723}{348951880031797248}, \frac{45574017678173074497482074500364087}{3780312033677803520}, \dots \right\}. \quad (149)$$

This is in agreement with equation (100) and an improvement compared to the WKB results of [52]. Again, the first six rational numbers are exact, followed by approximate ones.

## 10. Appendix C: First-Order Differential Equations for $E_n(g)$

Given a one-dimensional quantum system

$$(H_0 + g V)|n, g\rangle = E_n(g)|n, g\rangle \quad (150)$$

with Hamiltonian  $H = H_0 + g V$ , eigenvalues  $E_n(g)$  and eigenstates  $|n, g\rangle$  we consider an infinitesimal increase  $dg$  in the coupling constant  $g$ . The eigenvectors will undergo a small change:

$$|n, g + dg\rangle = |n, g\rangle + dg \sum_{k \neq n} u_{nk} |k, g\rangle \quad (151)$$

so that

$$\frac{d}{dg} |n, g\rangle = \sum_{k \neq n} u_{nk} |k, g\rangle. \quad (152)$$

Given this, we take the derivative of (150) with respect to  $g$  and multiply by  $\langle m, g|$  from the left to obtain:

$$\langle m, g|V - E'_n(g)|n, g\rangle = \sum_{k \neq n} u_{nk} \langle m, g|H_0 + g V - E_n(g)|k, g\rangle. \quad (153)$$

Setting now  $m = n$  and  $m \neq n$  in turn, we find:

$$E'_n(g) = V_{nn}(g) \quad (154)$$

$$V_{mn}(g) = u_{nm} (E_m(g) - E_n(g)), \quad (155)$$

where  $V_{mn}(g) = \langle m, g|V|n, g\rangle$ .

Equation (154) governs the behavior of the eigenvalues as functions of the coupling constant  $g$ . In order to have a complete system of differential equations, we must also determine how the  $V_{mn}(g)$  change, when  $g$  changes. With the help of equations (152) and (155), we obtain:

$$V'_{mn} = \sum_{k \neq m} u_{mk}^* \langle k, g|V|n, g\rangle + \sum_{k \neq n} u_{nk} \langle m, g|V|k, g\rangle \quad (156)$$

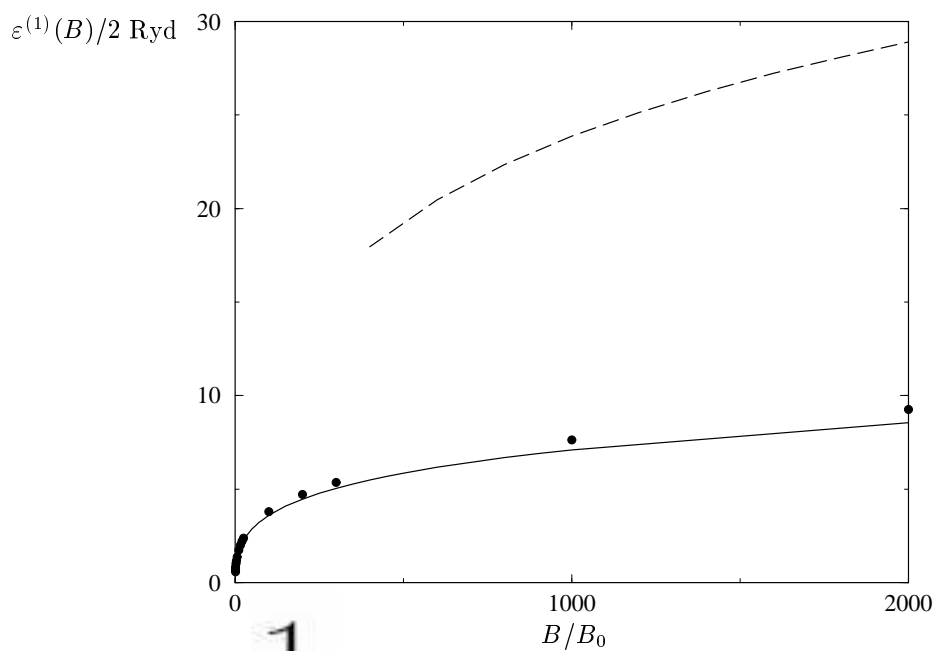
$$V'_{mn} = \sum_{k \neq m} \frac{V_{mk} V_{kn}}{E_m - E_k} + \sum_{k \neq n} \frac{V_{mk} V_{kn}}{E_n - E_k}. \quad (157)$$

Equations (154) and (157) together describe a complete set of differential equations for the energy eigenvalues  $E_n(g)$  and the matrix-elements  $V_{nm}(g)$ . The latter determine via (155) the expansion coefficients  $u_{nm}(g)$ . Initial conditions are given by the eigenvalues  $E_n(0)$  and the matrix elements  $V_{nm}(0)$  of the unperturbed system.

- [1] J. Goldstone, A. Salam, and S. Weinberg, Phys. Rev. **127**, 965 (1962).
- [2] C. De Dominicis, J. Math. Phys. **3**, 983 (1962).
- [3] R.P. Feynman, *Statistical Mechanics*, Benjamin, Reading, 1972.
- [4] R.P. Feynman and H. Kleinert, Phys. Rev. A **34**, 1986 (<http://physik.fu-berlin.de/~kleinert/159/159.pdf>).
- [5] H. Kleinert Phys. Lett. A **173**, 332 (1993) (<http://physik.fu-berlin.de/~kleinert/213>).
- [6] H. Kleinert, *Path Integrals in Quantum Mechanics, Statistics, Polymer Physics, and Financial Markets*, World Scientific, Singapore, 2009 (<http://www.physik.fu-berlin.de/~kleinert/b5>).
- [7] H. Kleinert, Annals of Physics **266**, 135 (1998) (<http://physik.fu-berlin.de/~kleinert/255/255.pdf>).
- [8] J.A. Lipa, D.R. Swanson, J.A. Nissen, T.C.P. Chui and U.E. Israelsson, Phys. Rev. Lett. —bf 76, 944 (1996); J.A. Lipa, D. R. Swanson, J.A. Nissen, Z.K. Geng, P.R. Williamson, D.A. Stricker, T.C.P. Chui, U.E. Israelsson and M. Larson, Phys. Rev. Lett. —bf 84, 4894 (2000).
- [9] H. Kleinert, Phys. Rev. D **60**, 085001 (1999) (hep-th/9812197) (hep-th/9812197); Phys. Lett. A **277**, 205 (2000) (cond-mat/9906107).
- [10] P.M. Stevenson, Phys. Rev. D **30**, 1712 (1985); D **32**, 1389 (1985); P.M. Stevenson and R. Tarrach, Phys. Lett. B **176**, 436 (1986).
- [11] W. Janke, H. Kleinert, Phys. Rev. Lett. **75**, 2787 (1995) (quant-ph/9502019).
- [12] E.J. Weniger, Phys. Rev. Lett. **77**, 2859 (1996); see also F. Vinette and J. Čížek, J. Math. Phys. **32**, 3392 (1991).
- [13] H. Kleinert and W. Janke, Phys. Lett. A **206**, 283 (1995) (quant-ph/9509005).
- [14] R. Guida, K. Konishi, H. Suzuki, Ann. Phys. (N.Y.) **249**, 109 (1996).
- [15] H. Kleinert, Phys. Rev. D **57**, 2264 (1998) (cond-mat/9801167); Phys. Rev. D **58**, 107702 (1998) (cond-mat/9803268).
- [16] B. Hamprecht and H. Kleinert, Phys. Rev. D **68**, 065001 (2003) (hep-th/0302116).
- [17] R. Seznec and J. Zinn-Justin, J. Math. Phys. **20**, 1398 (1979). This paper has developed important techniques for understanding the convergence mechanism of variational perturbation theory.
- [18] H. Kleinert and V. Schulte-Frohlinde, *Critical Phenomena in  $\Phi^4$ -Theory*, World Scientific, Singapore, 2001 (<http://www.physik.fu-berlin.de/~kleinert/b8>).
- [19] J. Zinn-Justin, *Quantum Field Theory and Critical Phenomena*, Clarendon, Oxford, 1989.
- [20] See Section 19.4 in [18].
- [21] F.J. Wegner, Phys. Rev. B **5**, 4529 (1972); B **6**, 1891 (1972).
- [22] B.G. Nickel, D.I. Meiron, and G.B. Baker, Univ. of Guelph preprint 1977 (unpublished). The preprint is readable on the WWW at <http://www.physik.fu-berlin.de/~kleinert/nickel/guelph.pdf>; The results are cited and used in Chapters 19 and 20. They were extended to seven loops by D.B. Murray and B.G. Nickel, Univ. of Guelph preprint 1991. The additional  $g^7$  coefficients of the renormalization group functions are listed in Section 20.4 of the textbook [18].
- [23] See Section 20.2 in [18].
- [24] H. Kleinert, Phys. Rev. D **60**, 085001 (1999) (hep-th/9812197). See Fig. 9.
- [25] M. Holzmann, G. Baym, J.-P. Blaizot and F. Laloë, Phys. Rev. Lett. **87**, 120403 (2001).
- [26] P. Arnold, G. Moore and B. Tomásik, cond-mat/0107124.
- [27] J. Zinn-Justin, *Quantum Field Theory and Critical Phenomena* (Oxford University Press, Oxford, England, 1996).
- [28] M. Bijnlsma and H. T. C. Stoof, Phys. Rev. A **54**, 5085 (1996)
- [29] F.F. de Souza Cruz, M.B. Pinto and R.O. Ramos, Phys. Rev. A **65**, 053613 (2002) (cond-mat/0112306).

- [30] E. Braaten, and E. Radescu, (cond-mat/0206186).
- [31] These are the results of [30]. They differ from those of Refs. [29] which are  $a_3 = 0.644519$ ,  $a_{41} = 0.87339$ ,  $a_{42} = 3.15905$ ,  $a_{43} = 1.70959$ ,  $a_{44} = 4.4411$ ,  $a_{45} = 2.37741$ . The coefficients of the series (57) to be resummed differ mainly in the last term:  $f_{-1} = -126.651 \cdot 10^{-4}$ ,  $f_0 = 0$ ,  $f_1 = -4.04857 \cdot 10^{-4}$ ,  $f_2 = 2.40587 \cdot 10^{-4}$ ,  $f_3 = -2.06849 \cdot 10^{-4}$ .
- [32] H. Kleinert, *Strong-Coupling Behavior of  $\Phi^4$ -Theories and Critical Exponents*, Phys. Rev. D **57**, 2264 (1998); Addendum: Phys. Rev. D **58**, 107702 (1998) (cond-mat/9803268); *Seven Loop Critical Exponents from Strong-Coupling  $\phi^4$ -Theory in Three Dimensions*, Phys. Rev. D **60**, 085001 (1999) (hep-th/9812197); *Theory and Satellite Experiment on Critical Exponent  $\alpha$  of Specific Heat in Superfluid Helium* Phys. Lett. A **277**, 205 (2000) (cond-mat/9906107).
- [33] H. Kleinert, *Strong-Coupling  $\phi^4$ -Theory in  $4 - \epsilon$  Dimensions, and Critical Exponent*, Phys. Lett. B **434**, 74 (1998) (cond-mat/9801167); *Critical Exponents without beta-Function*, Phys. Lett. B **463**, 69 (1999) (cond-mat/9906359).
- [34] See [29, 30, 41] and references cited there.
- [35] With standard normalization conditions used in the 3-dimensional  $\phi^4$ -theory, the approach to scaling is governed by Wegner's exponent  $\omega$  (see [32]). The present definition of  $m$  differs from the inverse correlation length  $m = \xi^{-1}$  by a factor:  $m = mZ_\phi^{-1} \propto m m^{-\eta/2}$  for  $m \rightarrow 0$ . This changes the exponent of approach to  $\omega' = \omega/(1 - \eta/2)$ . I thank B. Kastening for noting this.
- [36] P. Arnold and G. Moore, Phys. Rev. Lett. **87**, 120401 (2001); Phys. Rev. E **64**, 066113 (2001). The authors derive a  $1/N$  correction factor  $(1 - 0.527/N)$  to the leading  $N \rightarrow \infty$  result.
- [37] V.A. Kashurnikov, N.V. Prokof'ev and B.V. Svistunov, Phys. Rev. Lett. **87**, 120402 (2001).
- [38] G. Baym, J.-P. Blaizot M. Holzmman, F. Laloë and D. Vautherin, Phys. Rev. Lett. **83**, 1703 (1999).
- [39] G. Baym, J.-P. Blaizot and J. Zinn-Justin, Europhys. Lett. **49**, 150 (2000).
- [40] P. Arnold and B. Tomášik, Phys. Rev. A **62**, 063604 (2000). This paper starts out from the 3+1-dimensional initial theory and derives from it the three-dimensional effective classical field theory, the field-theoretic generalization of the quantum-mechanical effective classical potential of R.P. Feynman and H. Kleinert, Phys. Rev. A **34**, 5080 (1986). This reduction program was started for the Bose-Einstein gas by A.M.J. Schakel, Int. J. Mod. Phys. B **8**, 2021 (1994); J. Mod. Phys. B **8**, 2021 (1994); *Boulevard of Broken Symmetries*, Habilitationsschrift, FU-Berlin, (cond-mat/9805152) (1998). Unfortunately, Schakel did not go beyond the one-loop level so that he was happy to have found a positive shift  $\Delta T_c/T_c$ , and did see the cancellation at the two-loop level. See his recent paper in J. Phys. Stud. **7**, 140 (2003) (cond-mat/0301050).
- [41] F.F. de Souza Cruz, M.B. Pinto and R.O. Ramos, Phys. Rev. B **64**, 014515 (2001).
- [42] P. Grueter, D. Ceperley, F. Laloe, Phys. Rev. Lett. **79**, 3549 (1997) (cond-mat/9707028).
- [43] See Eq. (20.23) in the textbook [18] or S.E. Derkachov, J.A. Gracey, and A.N. Manashov, Eur. Phys. J. C **2**, 569 (1998) (hep-ph/9705268).
- [44] W. Janke and H. Kleinert, Phys. Lett. A **117**, 353 (1986) <http://www.physik.fu-berlin.de/~kleinert/133>; Phys. Rev. Lett. **58**, 144 (1986). H. Kleinert, Phys. Lett. A **257**, 269 (1999) (cond-mat/9811308); M. Bachmann, H. Kleinert, A. Pelster, Phys. Lett. A **261**, 127 (1999) (cond-mat/9905397); Physical Review E **63**, 051709/1-10 (2001) (cond-mat/0011281); see also B. Kastening, Phys. Rev. A **68**, 061601 (2003) (cond-mat/0303486); Phys. Rev. A **69**, 043613 (2004) (cond-mat/0309060); Phys. Rev. E **73**, 011101 (2006) (cond-mat/0508614); Phys. Rev. A **70**, 043621 (2004) (cond-mat/0406035).
- [45] J.S. Langer, Ann. Phys. **41**, 108 (1967).
- [46] C.M. Bender and T.T. Wu, Phys. Rev. **184**, 1231 (1969);
- [47] S. Coleman, Nucl. Phys. B **298**, 178 (1988).
- [48] B. Bellet, P. Garcia, A. Neveu, Int. J. of Mod. Phys. A **11**, 5587 (1997)
- [49] J.-L. Kneur, D. Reynaud, (hep-th/0205133v2). See also [50], [29], [41].
- [50] E. Braaten, E. Radescu, (cond-mat/0206186v1).
- [51] The low-order results were first obtained by H. Kleinert, Phys. Lett. B **300**, 261 (1993) (<http://www.physik.fu-berlin.de/~kleinert/214>), and extended by R. Karrlein and H. Kleinert, Phys. Lett. A **187**, 133 (1994) (hep-th/9504048).
- [52] J. Zinn-Justin, J. Math Phys. **22**(3), 511 (1981). The first 10 coefficients of expansion (99) are calculated.
- [53] B. Bellet, P. Garcia, A. Neveu, Int. J. of Mod. Phys. A **11**, 5587 (1997). The family structure of optimal variational parameters emphasized in this paper was discussed in great detail earlier in Chapter 5 of the textbook [6], but with correct application rules.
- [54] M. Bachmann, H. Kleinert, and A. Pelster, Phys. Rev. A **62**, 52509 (2000) (quant-ph/0005074), Phys. Lett. A **279**, 23 (2001) (quant-ph/000510).
- [55] J.E. Avron, B.G. Adams, J. Čížek, M. Clay, M.L. Glasser, P. Otto, J. Paldus, and E. Vrscaj, Phys. Rev. Lett. **43**, 691 (1979).
- [56] L.D. Landau and E.M. Lifschitz, *Quantenmechanik*, Sechste Auflage (Akademie-Verlag Berlin, 1979).
- [57] J.E. Avron, I.W. Herbst, B. Simon, Phys. Rev. A **20**, 2287 (1979). See also the resummation treatment in J.-C. Le Guillou, J. Zinn-Justin, Ann. Phys. **147**, 57 (1983).
- [58] H. Ruder, G. Wunner, H. Herold, and F. Geyer, *Atoms in Strong Magnetic Fields* (Springer-Verlag, Berlin, 1994).
- [59] G. Ahlers, Phys. Rev. A **3**, 696 (1971); K.H. Mueller, G. Ahlers, F. Pobell, Phys. Rev. B **14**, 2096 (1976);
- [60] L.S. Goldner, N. Mulders and G. Ahlers, J. Low Temp. Phys. **93** (1992) 131.
- [61] R. Guida and J. Zinn-Justin, *Critical exponents of the N-vector model*, J. Phys. A **31**, 8130 (1998) (cond-mat/9803240)
- [62] J.C. Le Guillou and J. Zinn-Justin, Phys. Rev. Lett. **39**, 95 (1977); Phys. Rev. B **21**, 3976 (1980); J. de Phys. Lett **46**, L137 (1985).
- [63] H. Kleinert and V. Schulte-Frohlinde, J. Phys. A **34**, 1037 (2001) (cond-mat/9907214).
- [64] D.B. Murray and B.G. Nickel, unpublished.
- [65] A. Pellissetto and E. Vicari, preprint IFUP-TH 52/97, cond-mat/9711078.
- [66] F. Jasch and H. Kleinert, Berlin preprint 199 (cond-mat/9907214).
- [67] W. Janke, Phys. Lett. A **148** (1990) 306.
- [68] H.G. Ballesteros, L.A. Fernandez, V. Martin-Mayor and A. Munoz Sudupe, Phys. Lett. B **387**, 125 (1996).
- [69] M. Ferer, M.A. Moore, and M. Wortis, Phys. Rev. B **65**, 2668 (1972).
- [70] P. Butera and M. Comi, Phys. Rev. B **56**, 8212 (1997) (hep-lat/9703018).





$$\begin{aligned}
 F^4 = & \frac{1}{2} \text{O} + 3 \text{O} \text{O} + 15 \text{O} \text{O} \text{O} \\
 & + 105 \text{O} \text{O} \text{O} + \frac{1}{2} (540 \\
 & + \frac{1}{6} \left( 1728 \text{O} \text{O} \text{O} + 3456 \text{O} \text{O} \text{O} + \right.
 \end{aligned}$$

$$F^4 = \frac{1}{2} \bigcirc + 3 \bigcirc \bigcirc + 15 \text{ (figure-eight) }$$

$$+ 105 \text{ (four-leaf clover) } + \frac{1}{2} (540$$

